This is to certify that the

thesis entitled

INDUCED CARBONATE PRECIPITATION AND CATION EXCHANGE IN SANDY AQUIFER SOLIDS

presented by

Lance B. Warnick

has been accepted towards fulfillment
of the requirements for

M.S. degree in Environmental Engr.

Craig S. Criddle
Major professor

Date 8/5/98

DATE DUE	DATE DUE	DATE DUE
1115 01 DEC 04 200 JUL 26 2006		
APR 01 2006		
SEP 25 2006 MAR 18 2007		
040810		

INDUCED CARBONATE PRECIPITATION AND CATION EXCHANGE IN SANDY AQUIFER SOLIDS

By

Lance B. Warnick

A THESIS

Submitted to
Michigan State University
in partial fulfillment of the requirements
for the degree of

MASTER OF SCIENCE

Department of Civil and Environmental Engineering

1998

ABSTRACT

INDUCED CARBONATE PRECIPITATION AND CATION EXCHANGE IN SANDY AQUIFER SOLIDS

By

Lance B. Warnick

Pseudomonas stutzeri strain KC (PKC) is a denitrifying bacterium that is capable of degrading CCl_4 without producing harmful degradation-by-products like chloroform. Researchers from Michigan State University in cooperation with the Michigan Department of Environmental Quality have been working to develop and implement an *in situ* bioremediation process capable of removing dissolved carbon tetrachloride (CCl_4) present in an aquifer in Schoolcraft, Michigan. However, alkali must be injected into the aquifer in order to raise the groundwater pH and create conditions favorable for CCl_4 transformation by PKC.

Carbonate precipitation and cation exchange are important mechanisms that help control groundwater chemistry and the rate of pH change as alkali is added to the aquifer. The potential for geochemical interaction of aquifer solids and the composition of groundwater samples from the Schoolcraft Aquifer were evaluated to establish baseline conditions before pH adjustment. Secondly, the addition of alkali to the aquifer and the resulting pH change were simulated using one-dimensional bench-scale experiments and the geochemical calculation program PHREEQC.

To Blondie and Bug.

ACKNOWLEDGEMENTS

This thesis could not have been possible without the help and guidance of my advisor, Dr. Craig Criddle. His experience and practical advice helped me accomplish many things that appeared impossible. Many times when I felt overwhelmed he helped me realize that I could "eat the whole cow—one piece at a time".

My wife, Melissa, supported me and encouraged me to continue even after many late nights at the lab, when nothing seemed to go right. She also sacrificed time for many of her own interests during the preparation of this thesis. My parents also helped prepare me for my education through their example of hard work and for helping me develop a love for hard work and an appreciation for the world around us all.

I would also like to thank Dr. Michael Dybas (MSU), who taught me many practical aspects of environmental fieldwork and Mr. Yan Pan (MSU), who spent many hours teaching me how to use the ICP-AES and IC and also analyzed countless samples. I would also like to thank the Michigan Department of Environmental Quality for funding my research as part of the Schoolcraft Bioaugmentation Experiment.

TABLE OF CONTENTS

LIST OF TABLES

LIST OF FIGURES

LIST OF ABBREVIATIONS

1-D ..... one-dimensional
^3H ..... tritium
Al ..... aluminum
ANC ..... acid neutralizing capacity
ASTM ..... American Society for Testing and Materials
Ba ..... barium
BEC ..... base-exchange capacity
bgs ..... below ground surface
BNC ..... base neutralizing capacity
Ca ..... calcium
$CaCl_2$ ..... calcium chloride
$CaCO_3$ ..... calcium-carbonate, calcite, or aragonite
$CaMg(CO_3)_2$ ..... dolomite
CaOH ..... calcium hydroxide
CCl_4 ..... carbon tetrachloride
CEC ..... cation-exchange capacity
Cl ..... chloride
cm ..... centimeter
Cu ..... copper
DDW ..... distilled deionized water
F ..... fluoride
Fe ..... iron
ft ..... foot or feet
g ..... gram
HCO_3 ..... bicarbonate
Hfo ..... hydrous ferric oxides
IC ..... ion chromatography
ICP-AES ..... inductively coupled plasma-atomic emission spectrometry
K ..... potassium
M ..... molar
MDEQ ..... Michigan Department of Environmental Quality
MDL ..... method detection limit
meq ..... milliequivalent
Mg ..... magnesium
mg ..... milligram
mL ..... milliliter
Mn ..... manganese
MSU ..... Michigan State University
N ..... normal

Na ..... sodium
NaF ..... sodium fluoride
NaOH ..... sodium hydroxide
Ni ..... nickel
No. ..... number
NO_3 ..... nitrate
OH ..... hydroxide
Pb ..... lead
PKC ..... *Pseudomonas stutzeri* strain KC
PVE ..... pore volumes exchanged
rpm ..... revolutions per minute
SAC ..... chemical surface adsorption capacity
SI ..... saturation indices
SiO_2 ..... silica or quartz
SO_4 ..... sulfate
Sr ..... strontium
$SrCl_2$ ..... strontium chloride
Zn ..... zinc
µL ..... microliter

CHAPTER 1

INTRODUCTION

1.0 Background

Research on the chemical interactions between groundwater and aquifer solids due to changes in groundwater pH has been limited. Historically, most of the research in the area of subsurface pH modification has been related to agriculture. Soil scientists have worked to understand how to control the pH of soil, in order to make nutrients more available to plants and limit the toxicity of trace metals. Lime (CaOH) is typically added to acidic soils in order to raise the pH and reduce the concentration of metals below toxic levels. The amount of base needed to raise the pH of a soil may be estimated using information about the soil and water chemistry.

When acid or alkali is added to most soils and waters, the pH does not immediately change due to buffering reactions in the solid (soil) and aqueous (water) phases. Therefore, the total neutralizing capacity of a soil/water system must therefore include contributions from both solid and aqueous phases. The terms acid neutralizing capacity (ANC) and base neutralizing capacity (BNC) describe the buffering capacity of soil/water systems (Ulrich and Sumner, 1991).

1.1 Geochemical processes

There are three types of processes that may occur as the pH of a soil/water system is modified. These processes include physical, chemical, and electrostatic interactions between the soil and water. Physical processes will not be discussed this thesis, however important chemical and electrostatic processes are affected as the pH of a solution changes. Three specific types of chemical and electrostatic processes that may be affected by altering pH include:

- Mineral equilibria (chemical),
- Cation exchange (electrostatic), and
- Chemical adsorption (chemical).

A brief description of each process in provided in subsequent sections.

1.1.1 Mineral equilibria

Mineral equilibria involve chemical processes like precipitation and dissolution that control the pH and concentration of ions in solution. When the concentration of a specific combination of ions exceeds the solubility capacity of a water system, the ions may precipitate from solution. The mineral may continue to precipitate and as long as the mineral solubility capacity of the solution is exceeded. However, if a geochemical change occurs that causes the solution to become undersaturated with respect to a specific mineral (e.g., decrease in solution pH), the mineral may then dissolve until the concentration of ions reaches an equilibrium concentration in solution. Equations showing the impact of pH on carbonate mineral equilibria are included in Appendix A.

Changing the pH of a solution is one way to impact or control the precipitation or dissolution of some carbonate minerals in solution. In fact, the pH of most natural waters is controlled by the precipitation and dissolution of carbonate minerals (Drever, 1997). As pH of a solution increases, carbonate minerals may form and precipitate from solution. An illustration showing the precipitation of a calcium carbonate mineral is included as Figure 1-1.

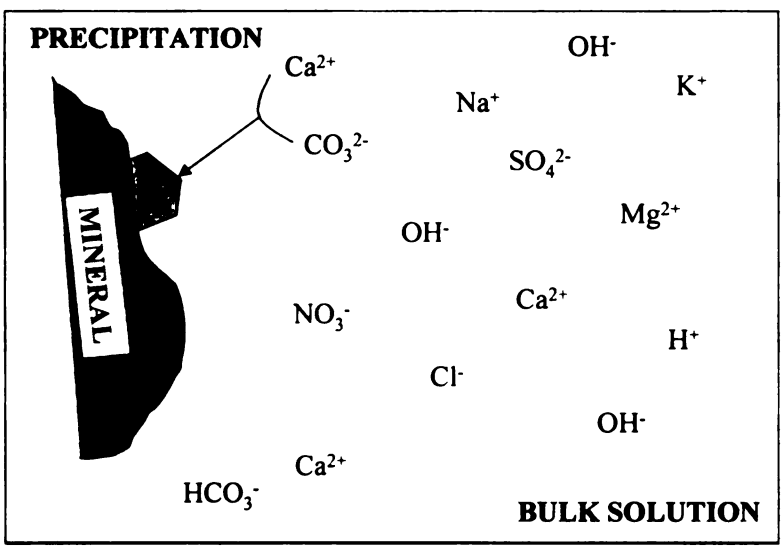

Figure 1-1. Mineral precipitation and dissolution

As shown in Figure 1-1, ions in solution can combine to form compounds that may precipitate from solution. The potential for pH-induced mineral precipitation in Schoolcraft groundwater is discussed in Chapters 4, 5, and 6.

1.1.2 Cation exchange

Cation exchange is an electrostatic interaction between the surface of solids and the surrounding solution. The potential of a solid to participate in cation exchange is defined as its cation exchange capacity (CEC). Silica (SiO_2), which is one of the most common minerals in soil, typically has an electrically charged surface, which can create electrostatic forces that may result in cation exchange occurring. When SiO_2 is exposed to water, these charged sites may dissociate and form hydroxide (OH^-) groups that produce a net negative charge on the mineral surface. Cations from the surrounding solution are attracted to OH^- groups and form a net positively charged layer in an effort to neutralize negative charge on the surface of the SiO_2. These cations (sometimes called counter-ions) may exchange with cations present in solution as pH or water chemistry changes. Figure 1-2 is an illustration of cation exchange occurring on the surface of a mineral.

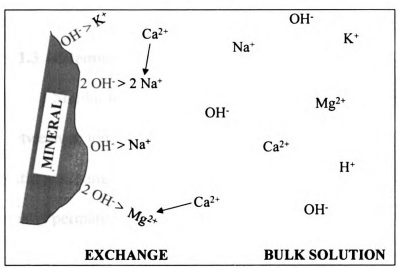

Figure 1-2. Cation exchange

As shown in Figure 1-2, calcium (Ca^{2+}) ions are exchanging with magnesium (Mg^{2+}) and sodium (Na^{+}) ions on the surface of a mineral. Although it is not shown in Figure 1-2, cation exchange may also occur between cations and protons adsorbed to the OH^{-} groups on the surface of solids. Divalent cations like Ca^{2+} and Mg^{2+} typically have a greater adsorption affinity than monovalent cations like Na^{+} and potassium (K^{+}). Generally, cations that are lower on the periodic table have a greater adsorption affinity than cations higher on the periodic table (e.g., $Ca^{2+} > Mg^{2+}$ and $K^{+} > Na^{+}$). However, the specific cations that form on a mineral's exchange complex depend on the type and concentration of cations in solution.

Cation exchange in a soil/water system can be influenced or controlled by several methods, including increasing solution pH or changing the composition or concentration of cations in solution. Equations showing the mechanisms involved in cation exchange are included in Table A-4 in Appendix A.

1.1.3 Chemical adsorption

Similar to cation exchange, chemical adsorption refers to a bonding process between an ion and a mineral surface. However, unlike the electrostatic bonds for cation exchange, the chemical bonds that form during chemical adsorption may be nearly permanent. Chemical adsorption of heavy and trace metals to soils is one reason the aqueous concentration of metals is typically much lower than expected (Drever, 1997). As groundwater pH increases, trace metal adsorption generally

impacts the only the concentration of metals in solutions, but not the major geochemical interactions between soil and water. Equations showing the mechanisms involved in chemical adsorption are included in Table A-5 in Appendix A.

1.2 Groundwater systems

In aquifers, as in any soil/water system, the total buffering capacity includes both contributions from both the solid (minerals) and aqueous (groundwater) phases. Appelo (1994) showed that even in extremely sandy soils mineral equilibria and ion exchange play important roles in controlling changes to groundwater chemistry. Environmental factors like pH, solution chemistry, contact time, and temperature, to name a few, may also control both the magnitude and involvement of each geochemical process. Pratt (1961) and Griffioen (1993) both demonstrated that the CEC of soils is a function of the pH of the system (i.e., CEC increases with increasing pH). Therefore the involvement of each of these processes (i.e., mineral equilibria, cation exchange, and chemical adsorption) on pH change must be evaluated for the site-specific conditions of a particular aquifer.

1.3 Schoolcraft Field Bioaugmentation Experiment

For the past several years, researchers from Michigan State University (MSU), in cooperation with the Michigan Department of Environmental Quality

(MDEQ), have been working to develop and implement an *in situ* process capable of removing dissolved carbon tetrachloride (CCl_4) present in an aquifer in Schoolcraft, Michigan. *In situ* bioremediation using the bacterium, *Pseudomonas stutzeri* strain KC (PKC), was selected as the preferred remedial approach. PKC is a denitrifying bacterium capable of degrading CCl_4 without producing harmful degradation-by-products like chloroform (Criddle et al., 1990; Tatara et al., 1993; Lewis et al., 1993; Dybas et al., 1995). Other microorganisms also have the ability to transform CCl_4, but chloroform is typically produced under denitrifying conditions.

The high nitrate concentrations present in the Schoolcraft Aquifer (see Chapter 3) create a situation that ideal for PKC, however iron-limiting conditions are required for rapid transformation of dissolved CCl_4 (Criddle et al., 1990; Tatara et al., 1993). One way of creating iron-limiting conditions in groundwater is by increasing pH, through the addition of an alkali (base). As the groundwater pH increases, dissolved iron becomes less soluble and precipitates out of solution (see Section 1.1.1). The lower iron concentrations, which result from this mineral precipitation, allow PKC to compete for food and nutrients with other microorganisms in an aquifer. The geochemical changes that occur as groundwater pH increases may have significant impacts on both the composition and/or reactivity of aquifer solids and CCl_4 transformation by PKC.

1.4 Experimental approach

In order to evaluate the potential impact of each of the three geochemical processes (mineral equilibria, cation exchange, and chemical adsorption), the capacity and degree of involvement of each process must be quantified. A series of one-dimensional (1-D) column experiments were used to simulate the addition of base to a soil/water system. Water present in the pore spaces of the aquifer solids was displaced by alkaline water (solution with a positive ANC) that was injected into the columns. Just as with any other plug flow reactor, the displaced water had little chance to mix and react with the bulk of the displacing solution. However, reactions immediately began to occur between the alkaline water and solid phase in an effort to reach a new chemical equilibrium. Under these conditions, cations present in the alkaline water may leave solution and be stored on the soil exchange complex and/or precipitate as the solubility of minerals are exceeded (Ulrich and Sumner, 1991).

The geochemical changes that occurred on the solids and in the groundwater were monitored and are presented in subsequent chapters and the appendices. This thesis evaluates that involvement of each of these processes on Schoolcraft solids and groundwater as the pH increased due to base addition.

CHAPTER 2

SCHOOLCRAFT AQUIFER SOLIDS

2.0 Introduction

Groundwater is continually seeking to equilibrate with the minerals that compose an aquifer. Depending upon the pH and geochemistry of the surrounding solution, these minerals may:

- Precipitate or dissolve (mineral equilibria),
- Act as ion exchangers (cation exchange), or
- Act as adsorption sites for metals (chemical adsorption).

The impact of each of these mechanisms during the pH-adjustment of groundwater was experimentally determined by comparing the properties of pH-adjusted solids with untreated solids that served as a control (see Chapter 6 and Appendices B and E). This section summarizes the geologic framework and baseline conditions of the solids that compose the Schoolcraft Aquifer.

2.1 Geologic framework

The Schoolcraft Aquifer is unconfined and composed of unconsolidated, glacial deposits (USGS, 1990). The aquifer solids are primarily fine- to medium-grain sand with occasional silt and clay regions (SFBE, 1997). The top of the water table is about 15 feet below ground surface (bgs) and the average saturated thickness of the aquifer ranges from 70 to 90 feet (Mayotte, et. al., 1996). The aquifer porosity is approximately 25 % and the hydraulic conductivity in the

aquifer is approximately 10^{-1} to 10^{-2} centimeters per second (cm/s), yielding a groundwater flow velocity of about 15 centimeters per day (cm/day) (Mayotte, et. al., 1996).

2.2 Aquifer mineralogy

In order to identify the major minerals that compose the aquifer, one sample of Schoolcraft aquifer solids collected from soil boring, SB-8, at a depth of about 71 feet. SB-8 is located several hundred feet upgradient from the region of the aquifer targeted for biotreatment using PKC. The locations of SB-8, well MW34A (discussed in subsequent sections), and the PKC biotreatment zone in relation to the CCl_4 plume in Schoolcraft, Michigan are shown on Figure 2-1.

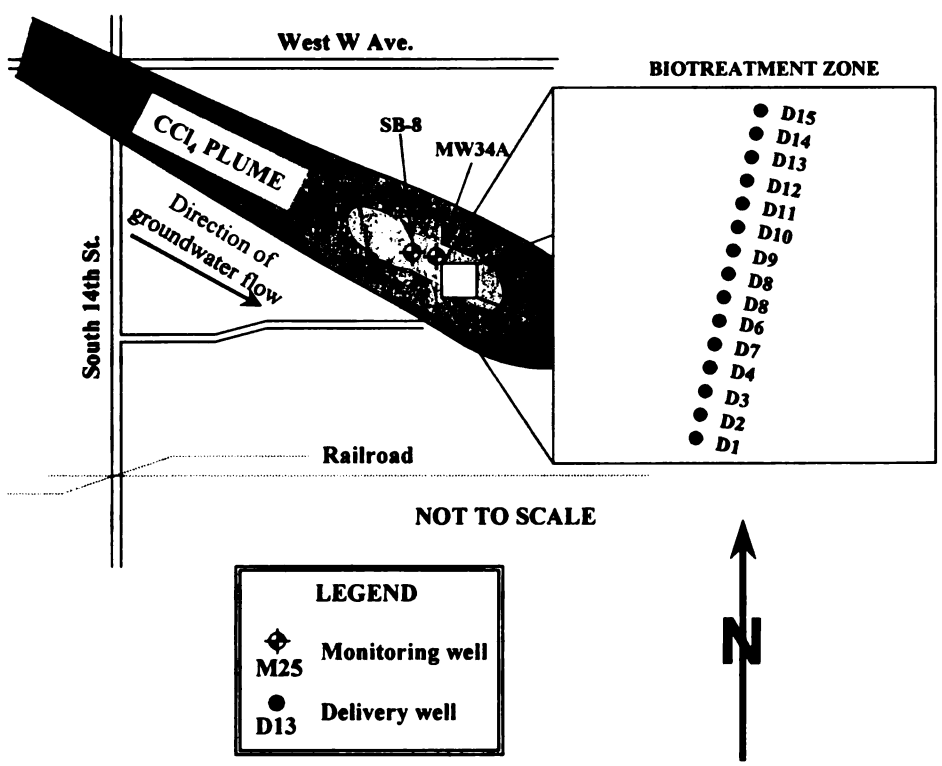

Figure 2-1. Sampling locations in the Schoolcraft (Michigan) Aquifer

The mineral grains were mounted on a slide, polished, and then examined under a petrographic microscope for light refraction, color, shape, cleavage, and crystalline form (SSSA, 1986). These observations enabled identification of the specific minerals that compose the individual grains. The grains were grouped into the following three classifications:

- Silicates (including quartz, feldspar, schist, and rock fragments),
- Calcite, and
- Dolomite.

Although, some of the grains contained more that one mineral, each grain was classified according to which mineral was most abundant. Results from the petrographic observations are included in Table 2-1.

Table 2-1. Mineral composition of Schoolcraft aquifer solids (Sibley, 1997)

Mineral	Percent (%)
Silicates	90 ± 4
Calcite	6 ± 3
Dolomite	4 ± 3

As shown in Table 2-1, roughly 90% of the sample of aquifer solids from SB-8 are silicates and the remaining 10% are the carbonate minerals, calcite ($CaCO_3$) and dolomite ($CaMg(CO_3)_2$). While this one evaluation of aquifer solids does not even begin to describe the complete mineral composition of the aquifer it does provide general information on the type of minerals present in the aquifer. This information is useful when trying to predict which chemical processes may occur between the groundwater and aquifer solids as pH changes.

Silicates are relatively geochemically stable minerals in most pH regimes, while carbonate minerals typically serve as the primary pH buffer in near neutral pH systems (Ulrich and Sumner, 1991), like the Schoolcraft Aquifer. As discussed in Section 1.1.2, silica minerals may serve as a primary matrix for cation exchange. As will be illustrated in Chapters 4 and 5, calcite precipitation had a significant impact on pH response as base was added to the groundwater.

2.3 Grain texture

Samples of approximately 275 feet of aquifer solids (2-inch-diameter) were collected during the installation of 15 groundwater delivery wells in July 1997 using a Waterloo cohesionless soil sampler. These 15 wells (labeled D1 through D15, see Figure 2-1) were constructed to deliver base, nutrients, and PKC across a 50 foot section of the aquifer. This region referred to, as the biotreatment zone (see Figure 2-1) is the primary focus of the field-scale bioremediation activities discussed in Section 1.3. Core from six of the delivery wells (D2, D4, D6, D8, D10, and D14) were logged, photographed, and divided into homogeneous segments based upon the following visually observed differences in particle size or texture:

- Silty sand,
- Fine sand,
- Medium sand,
- Coarse sand, and
- Very coarse sand.

It should be noted that these classifications were based upon visual observations only and may not necessary be similar to formal classification methods that utilize sieves to determine particle texture (SSSA, 1986). A total of 79 core segments were examined and classified as shown in Table 2-2.

Table 2-2. Solids texture in 79 samples of Schoolcraft aquifer solids

Grain Texture	No. of Samples	Percent of Total
Silty sand	1	1.3
Fine sand	23	29.1
Medium sand	37	46.8
Coarse sand	17	21.5
Very coarse sand	1	1.3
Total	79	100

As shown in Table 2-2, fine-, medium-, and coarse-grained sands account for over 97 % of the total number of samples collected, since there was only one sample each of silty-sand and very-coarse-grained sand. These findings are similar to the historical description of aquifer minerals discussed in Section 2.1. Since the silty-sand and very-coarse-grained sand comprise less than 3 % of the total number of core samples, only the fine-, medium-, and coarse-grained sands will be discussed in subsequent sections. The relative position below ground surface of each of the core samples is shown on Figure 2-2.

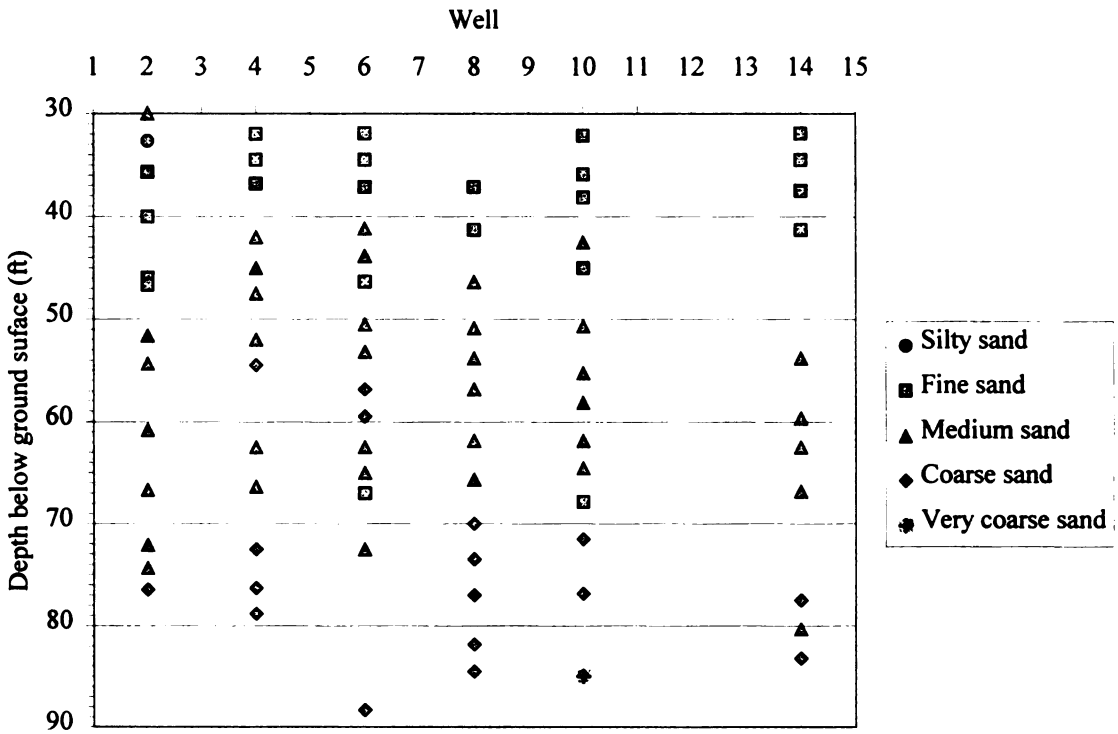

Figure 2-2. Observed particle size distribution in Schoolcraft aquifer cores

As shown in Figure 2-2, there are three observable layers of material in the aquifer near the 15 delivery wells. The aquifer is primarily fine-grained sand from 30 feet to 40 feet bgs, medium-grained sand from 40 feet to 70 feet bgs, and coarse-grained sand from 70 feet to 90 feet bgs. Solids samples were not collected in the clay layer that serves as a no-flow boundary at an average depth of 90 feet bgs. Figure 2-2 also shows that the sand layers are not entirely homogeneous, as indicated by the intermingling of other sand textures in the layers discussed above.

Each homogeneous core segment was also subdivided into smaller samples for characterization in terms of porosity, hydraulic conductivity, surface area, CCl_4 concentration, microbial characterization, and potential for geochemical

interaction. This thesis includes data only on the potential for geochemical interaction of the aquifer solids, and not the other parameters discussed above. The potential for geochemical interaction was defined in terms of:

- Solids pH,
- Base exchange capacity (BEC), and
- Chemical surface adsorption capacity (SAC).

2.4 Solids pH

The pH of Schoolcraft aquifer solids was measured using an Orion® SA 720 pH meter calibrated using two standard pH buffers (pH 7.00 ± 0.01 and pH 10.00 ± 0.01). The pH of aquifer solids was measured using two methods described in ASTM Standard D 4972-95a (ASTM, 1996). The methods were followed as outlined in the standard, except that in an effort to conserve the amount of solids for other experiments, only 5 grams (g) of solids and 5 milliliters (mL) of water were used instead of 10 g of solids and 10 mL of water. The first method used to measure solids pH involved measuring the pH in a soil/water slurry made using one part aquifer solids to one part distilled deionized water (DDW). The second method measuring the pH in a 0.01 molar (M) calcium chloride ($CaCl_2$) slurry made by adding one drop of 1 M $CaCl_2$ to the DDW slurry already prepared. The average pH of the aquifer core samples is shown in Table 2-3.

Table 2-3. Average pH of Schoolcraft aquifer solids

Grain Texture	No. of Samples	Solids pH in DDW	Solids pH in 0.01 M $CaCl_2$
Fine sand	23	9.2 ± 0.1	8.2 ± 0.1
Medium sand	36	9.4 ± 0.1	8.3 ± 0.1
Coarse sand	10	9.4 ± 0.1	8.2 ± 0.1

As shown in Table 2-3, there does not appear to be a statistical difference in the pH measured for the different grain textures of Schoolcraft aquifer solids. The similarity in pH values for the different grain textures of solids suggests that the initial ANC of the solids is similar. Table 2-3 also shows that the pH of solids measured in DDW (pH 9.1-9.5) was about one pH unit higher than the value measured in the 0.01 M $CaCl_2$ slurry (pH 8.1-8.4). This difference in pH readings is due to the increased concentration of ions resulting from adding the $CaCl_2$ solution. The presence of soluble salts in the DDW slurry may affect the pH readings. Adding $CaCl_2$ to the slurry helps reduce the impact of these soluble salts by increasing the total salt concentration (NCR, 1988). Soil scientists typically agree that solids pH values measured in the $CaCl_2$ solution are more representative of actual *in situ* pH values.

2.5 Base exchange capacity

The concentrations of four exchangeable bases, Ca^{2+}, Mg^{2+}, Na^{+}, and K^{+}, present on the cation exchange complex of Schoolcraft aquifer solids were measured using a strontium chloride ($SrCl_2$) displacement method modified from

Appelo (1990). Sr^{2+} was selected over other displacing cations (Na^+, K^+, and NH_4^+) since is behaves similar to both Ca^{2+} and Mg^{2+}, the main exchangeable cations in most types of soils (Sullivan, 1977).

A known mass of aquifer solids (approximately 3 g) was placed in a 15-mL plastic centrifuge tube with 10 mL of 0.25 M $SrCl_2$. The tube was shaken overnight on a shaker table to order to provide mixing between the solids and $SrCl_2$ solution. The concentration of Sr^{2+} in the 0.25 M $SrCl_2$ solution is typically a 100 times the concentration of Ca^{2+} in the groundwater that was equilibrated with the aquifer solids. The high concentration of Sr^{2+} in solution displaces cations (Ca^{2+}, Mg^{2+}, and K^+) from the surface of the aquifer solids and forces them into solution (see Figure 1-1). The sample was then centrifuged at 2,100 revolutions per minute (rpm) for 5 minutes to separate the solids from the liquids. The supernatant was decanted and analyzed for Ca^{2+}, Mg^{2+}, Na^+, and K^+ using inductively coupled plasma-atomic emission spectrometry (ICP-AES) (Method 3120 B, APHA, et. al., 1995).

One drawback with using $SrCl_2$ displacement to measure BEC is that the method does not correct for carbonate dissolution that may occur during displacement. The potential dissolution of calcium carbonate minerals during displacement may result in overestimating the amount of Ca^{2+} originally present on the surface exchange complex. In order to reduce the potential for carbonate dissolution, the pH of the $SrCl_2$ solution was maintained at or above pH 8, the point where calcite typically remains a precipitate.

The concentration of cations in the supernatant and the mass of the solids extracted were then used to calculate the BEC of the core samples. The average BEC of the Schoolcraft core samples (grouped by grain texture) is included in Table 2-4.

Table 2-4. Base exchange capacity of Schoolcraft aquifer solids

Grain Texture	No. of Samples	Ca^{2+} (meq/100 g)	Mg^{2+} (meq/100 g)	Na^{+} and K^{+} (meq/100 g)	Total (meq/100 g)
Fine sand	23	3.3 ± 1.8	0.29 ± 0.08	< 0.02	3.6 ± 1.9
Medium sand	37	3.5 ± 1.1	0.25 ± 0.05	< 0.02	3.8 ± 1.1
Coarse sand	17	3.7 ± 1.0	0.35 ± 0.26	< 0.02	4.1 ± 1.1

As shown in Table 2-4, Ca^{2+} occupies about one order-of-magnitude more cation exchange sites on the aquifer solids than Mg^{2+}. However, as will be illustrated in Chapters 4 and 5, both cations play important roles during groundwater pH adjustment. Table 2-4 shows the average total BEC ranges from 3.6 ± 1.9 millieqivalents (meq) per 100 g to 4.1 ± 1.1 meq/100 g indicating that there is little difference (approximately 12 %) in the BEC capacity measured for the three soil grain textures. The impact of Na^{+} and K^{+} on BEC in these core samples is considered to be negligible as indicated by the low concentrations of both cations (< 0.02 meq/100 g).

2.6 Chemical surface adsorption capacity

The potential for chemical adsorption is partly a function of the activity of surface exchange sites on the aquifer solids. The amount of chemical adsorption sites on the aquifer solids was measured using a sodium fluoride (NaF) displacement method (McBride, 1994). The number of reactive OH^- sites on the mineral surfaces is measured by monitoring the pH change in a concentrated NaF (approximately 1 M) solution after adding a known mass of soil. Fluoride (F^-) ions displace OH^- from the mineral surfaces and free OH^- ions cause the pH to increase. The number of OH^- ions displaced, as measured by the resulting increase in pH, corresponds to the amount of sites available for cation adsorption. The average SAC of the Schoolcraft core samples is shown in Table 2-5.

Table 2-5. Surface adsorption capacity of Schoolcraft aquifer solids

Grain Texture	No. of Samples	SAC (meq/100g)
Fine sand	13	9.4E-05
Medium sand	17	4.9E-05
Coarse sand	4	3.9E-05

As shown in Table 2-5, it appears that SAC decreases with increasing particle size (i.e., fine- to coarse-grained). Assuming that the concentration of surface exchange sites per unit area of a mineral is constant, the greater the surface area, the greater the number of surface exchange sites. Small particles like fine-grained sands have a larger surface per unit volume of material than coarse-grained sands

and therefore a greater SAC. The concentration of surface exchange sites is about five order of magnitude less that the concentration of base exchange sites (see Table 2-4), suggesting that BEC is a more important process when it comes to geochemical changes in Schoolcraft aquifer solids.

CHAPTER 3

SCHOOLCRAFT GROUNDWATER CHEMISTRY

3.0 Introduction

During the biotreatment phase of the Schoolcraft Field Bioaugmentation Project, NaOH was periodically injected into the aquifer in order to raise groundwater pH from about 7.2 to 8.2. The addition of NaOH has significant impacts on the geochemistry of the aquifer due to increased pH and concentration of Na^+ in solution. The water chemistry of the Schoolcraft Aquifer or any aqueous solution must be understood in order to predict and explain geochemical changes that occur as pH changes.

Chemical properties that were used to describe the composition of Schoolcraft groundwater include pH, alkalinity, and the concentration of major cations, SiO_2, major anions, and trace metals. The methods used to collect and quantify each of these properties in groundwater samples are outlined in the following sections.

3.1 Groundwater sampling

During September 1997, 81 groundwater samples were collected from monitoring locations in the biotreatment area of the Schoolcraft Aquifer. Dedicated in-well sample tubing and peristaltic pumps were used to collect samples from a network of multi-level monitoring wells shown on Figure 3-1.

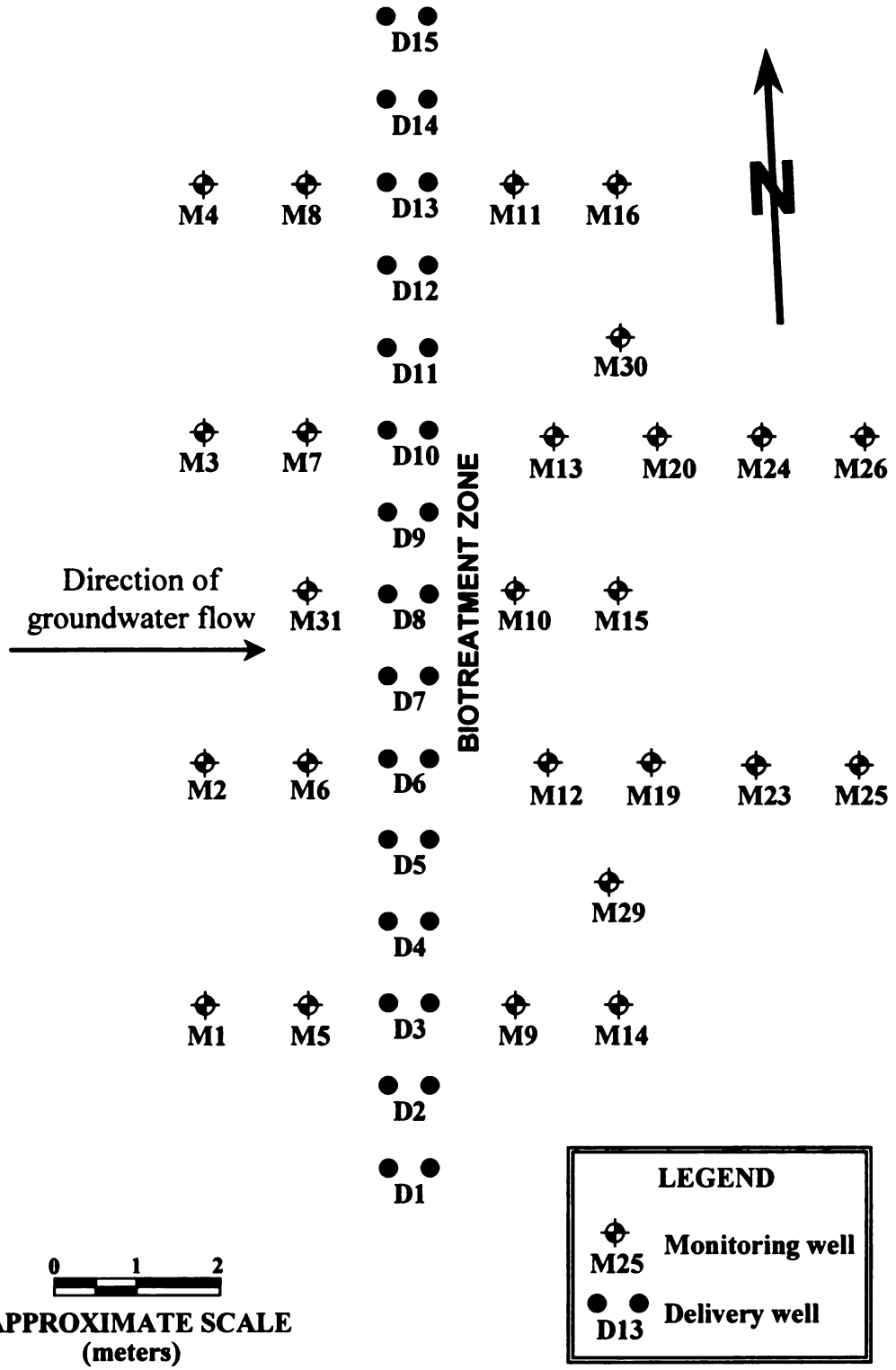

Figure 3-1. Location of monitoring wells near the biotreatment zone

Sixty-seven (67) of the 81 groundwater samples collected were used to characterize the pretreatment or *baseline* chemistry of the aquifer. The data for the remaining 14 samples were rejected due to equipment malfunction or analytical results being outside acceptable limits (see Section 3.7). The average value of each chemical property (e.g. pH, alkalinity, cation concentration) for the baseline groundwater samples are presented in the following sections.

3.2 Groundwater pH

The pH of Schoolcraft groundwater samples was measured using an Orion® SA 720 pH meter. The pH meter was calibrated between two standardized pH buffers (pH 7.00 ± 0.01 and pH 10.00 ± 0.01). The pH of each groundwater sample was measured immediately after collection in the field, or samples were sealed in plastic bottles with zero headspace, stored in a cooler at 4 degrees Celsius (°C), and transported to the laboratory for analysis. Typically, all pH measurements were performed within 10 hours of sample collection. The pH of all samples was recorded to the nearest hundredth (0.01) after the readings had stabilized. The average pH of the 67 baseline groundwater samples was determined to be 7.32 ± 0.03.

3.3 Alkalinity

At the average groundwater pH of 7.32, HCO_3^- is the only major component of alkalinity (Snoeyink and Jenkins, 1980). Alkalinity was quantified

by measuring the equivalents of a standardized acid required to lower a specific volume of groundwater to pH 4.5 (Method 2320 B, APHA, et. al., 1995). The standardized acid was dispensed using a Fisher® digital burette with a display precision of 0.01 mL. An Orion® SA 720 pH meter calibrated between two standard buffers (pH 4.00 ± 0.01 and pH 7.00 ± 0.01) was used to measure the pH of the titrated sample. The average alkalinity of the 67 baseline samples is 417 ± 26 milligrams per liter (mg/L) in terms of mass or 6.83 ± 0.42 milliequivalents per liter (meq/L) in terms of charge.

3.4 Major cations

Major cations are those that are present in relatively large concentrations or those that have significant impacts on the geochemistry of the system. The major cations in Schoolcraft groundwater include Ca^{2+}, Mg^{2+}, Na^{+}, and K^{+}. The concentration of each cation and SiO_2 in groundwater were measured ICP-AES, as discussed in Section 2-5 (Method 3120 B, APHA, et. al., 1995). The average concentrations of Ca^{2+}, Mg^{2+}, Na^{+}, K^{+}, and SiO_2, in the baseline groundwater samples are shown in Table 3-1.

Table 3-1. Major cations and silica in Schoolcraft groundwater

Chemical Property	No. of Samples	Concentration (mg/L)	Concentration (meq/L)	Percent of Positive Charge
Ca^{2+}	67	99.4 ± 9.5	4.95 ± 0.47	56.1
Mg^{2+}	67	31.7 ± 3.0	2.60 ± 0.24	29.4
Na^{+}	67	26.8 ± 8.9	1.16 ± 0.38	13.1
K^{+}	67	4.2 ± 2.2	0.10 ± 0.05	1.1
SiO_2	67	13.6 ± 1.6	Not applicable	Not applicable
		Total	8.83 ± 0.83	99.7

As shown in Table 3-1, Ca^{2+} accounts for 56.1 % of the total positive charge in the baseline Schoolcraft groundwater samples. Mg^{2+}, Na^{+}, and K^{+} provide 29.4 %, 13.1 %, and 1.1 % of total cationic charge. SiO_2 is a neutral compound and does not contribute a charge (positive or negative) to groundwater. Table 3-1 also shows that the sum of the positive charge resulting from major cations is 99.7 %. The sum of positive charges does not add up to 100 % due to rounding errors and neglecting standard deviations when calculating the percent of total positive charge.

3.5 Major anions

The major anions in Schoolcraft groundwater are bicarbonate (HCO_3^-), chloride (Cl^-), nitrate (NO_3^-), and sulfate (SO_4^{2-}). The concentrations of all anions, except HCO_3^-, were measured using ion chromatography (IC) as described in Standard Method: 4110 B (APHA, et. al., 1995). As discussed in Section 3.2, the

concentration of HCO_3^- was determined by measuring the alkalinity of the groundwater samples. The average concentrations of major anions (including HCO_3^-), in the baseline groundwater samples are shown in Table 3-2.

Table 3-2. Major anion concentrations in Schoolcraft groundwater

Major Anion	No. of Samples	Concentration (mg/L)	Concentration (meq/L)	Percent of Negative Charge
HCO_3^-	67	417 ± 26	6.83 ± 0.42	68.9
Cl^-	67	55.6 ± 15.1	1.56 ± 0.42	15.7
NO_3^-	67	54.1 ± 13.8	0.87 ± 0.22	8.8
SO_4^{2-}	67	30.8 ± 8.3	0.64 ± 0.17	6.5
		Total	9.92 ± 0.69	99.9

As shown in Table 3-2, HCO_3^- accounts for 68.9 % of the total negative charge in the baseline Schoolcraft groundwater samples. Cl^-, NO_3^-, and SO_4^{2-} provide 15.7 %, 8.8 %, and 6.5 % of total cationic charge. Table 3-2 also shows that the total negative charge resulting from major anions is 99.9 %. The sum of negative charges does not add up to 100 % due to rounding errors and neglecting standard deviations when calculating the percent of total negative charge.

3.6 Trace metals

The average concentrations of nine trace metals, aluminum (Al), barium (Ba), copper (Cu), iron (Fe), manganese (Mn), nickel (Ni), lead (Pb), strontium (Sr), and zinc (Zn), were also quantified using ICP-AES, as discussed in Section

2-5 (Method 3120 B, APHA, et. al., 1995). The average concentrations of the trace metals analyzed in the 67 baseline groundwater samples are shown in Table 3-3.

Table 3-3. Trace metals concentrations in Schoolcraft groundwater

Trace Metal	Samples Analyzed	Samples Above MDL	Concentration (mg/L)	Concentration (meq/L)
Al	67	62	0.16 ± 0.06	< 0.01
Ba	67	66	0.05 ± 0.01	< 0.01
Cu	67	0	< 0.03	< 0.01
Fe	67	6	0.19 ± 0.14	< 0.01
Ni	67	13	0.03 ± 0.01	< 0.01
Mn	67	14	0.07 ± 0.12	< 0.01
Pb	67	37	0.05 ± 0.03	< 0.01
Sr	67	67	0.12 ± 0.02	< 0.01
Zn	67	45	0.04 ± 0.01	< 0.01
			Total	< 0.10

The third column in Table 3-3 shows how many of the 67 baseline samples had concentrations above the method detection limit (MDL). Cu was the only trace metal analyzed that did not have measurable concentrations in any of the baseline groundwater samples. The concentration of Cu was reported as less than the MDL (i.e., < 0.03 mg/L). Table 3-3 also shows the charge concentration for each of the trace metals that were analyzed. All of the nine trace metals had charge concentrations less than 0.01 meq/L. The positive charge from all trace metals analyzed is less than 0.1 meq/L. When compared to the total positive charge in the groundwater samples (8.83 meq/L, see Table 3-1) the charge contribution, from the trace metals analyzed, is approximately 1 %.

The presence of trace metals in high concentrations may affect the activity and viability of microorganisms like PKC (Tatara et al., 1993). High concentrations of Zn (0.83 mg/L) were observed in groundwater samples collected in May 1997 from well MW34A (see Figure 2-1) for a bench-scale experiment. It was later determined, by reviewing field records, that the groundwater samples were collected before the steel-cased well was sufficiently purged.

PKC would not grow in any of these groundwater samples even though pH and food concentrations appeared ideal. A series of serial dilutions was performed to determine if high concentrations of Zn inhibited growth of PKC. After inoculation in diluted groundwater samples, PKC grew normally. These experiments help verify that the high concentrations of Zn were toxic to PKC.

It was hypothesized that the concentration of Zn in groundwater would decrease due to surface adsorption of the metals by the aquifer solids (see Figure 1-1 and Section 2.6) and enable PKC to grow in the groundwater. Approximately 1 g of Schoolcraft aquifer solids was placed in three 50-mL Erlenmeyer flasks with 10 mL of groundwater. The flasks containing the soil/water slurry and a control flask containing only 10 mL of groundwater were then placed on a shaker table operating at approximately 90 rpm, for three days. The slurry was centrifuged at 4,800 rpm for 30 minutes and the decanted supernatant was analyzed for trace metals using ICP-AES. The concentrations of Zn in the samples are shown in Table 3-4.

Table 3-4. Concentrations of Zn in groundwater exposed to aquifer solids

Sample No.	Before Exposure (mg/L)	After Exposure (mg/L)	Percent Decrease
1	0.80	< 0.01	> 98.8
2	0.93	0.03	96.8
3	0.88	0.03	96.6
Average	0.87 ± 0.07	0.02 ± 0.01	97.4

As shown in Table 3-4, the concentration of Zn decrease by an average 97.4% when the groundwater was exposed to Schoolcraft aquifer solids. The average concentration of Zn after exposure to aquifer solids (0.02 ± 0.01 mg/L) is about 50% less than the average concentration in the baseline samples (0.04 ± 0.01 mg/L, see Table 3-3). This decrease in the Zn concentration was due to adsorption of the trace metals on the surface sites of the aquifer solids (see Section 2-6). PKC inoculated into the groundwater exposed to aquifer solids grew normally without any further trace metal toxicity problems.

3.7 Charge balance

An aqueous solution must be electrically neutral in order for the system to be in equilibrium. As shown in Tables 3-1, 3-2, and 3-3, the concentration of each chemical constituent (cations, anions, and trace metals) was expressed in terms of both mass (mg/L) and charge (meq/L). Electroneutrality requires that the sum of the positive (cation) charges equal the sum of the negative (anion) charges. Analyses of the baseline groundwater samples that produced a cation-anion charge difference greater than 20 % were rejected and not included when characterizing

the groundwater chemistry. The average charge concentrations for major cations, anions, and trace metals in the baseline Schoolcraft groundwater samples are included in Table 3-5.

Table 3-5. Average concentration in Schoolcraft groundwater samples

Chemical Property	Cation Concentration (meq/L)	Anion Concentration (meq/L)
Major Cations	8.83 ± 0.83	N/A
Anions	N/A	9.92 ± 0.69
Trace Metals	< 0.10	N/A
Total	8.83 ± 0.83	9.92 ± 0.69

As shown in Table 3-5, the total cation concentration in 8.83 meq/L and the average total anion concentration is 9.92 meq/L. The ration of cation concentration to anion concentration is 8.83/9.92 or approximately 89 %, resulting in a charge difference of approximately 11 %. This 11 % cation-anion charge difference is within the 20 % acceptance criteria discussed earlier.

One reason for the 11 % difference in charge concentration is due to the fact that all these values are averages concentrations from 67 samples. Therefore the 11 % charge difference does not reflect values for all baseline samples. A cation-anion charge difference of only 1.5 % resulted from an evaluation of the groundwater chemistry from well MW34A (see Figure 2-1). This small error indicates that the analytical methods employed to quantify the concentration of

major cations and anions are adequate, and may be used describe some of major geochemical properties of Schoolcraft groundwater.

Another reason for the 11 % cation-anion charge difference is due to human error while performing alkalinity titrations (see Section 3.3). Due to the large concentration of alkalinity (6.83 meq/L, see Table 3-2), a strong acid was used to reduce the total volume of acid required for each titration. Even though the automatic burette is capable of delivering standardized acid to an accuracy of 0.01 mL, the operator may still unintentionally dispense more acid than needed to reach the pH 4.5 endpoint. One extra drop of 0.1 normal (N) acid will titrate the sample beyond the pH 4.5 endpoint, and if unaccounted, will cause the alkalinity of the sample to be overestimated.

3.8 Hydrochemical facies

Hydrochemical facies are classification schemes based on the dominant cation and/or anion in water (Wahrer, 1993). A cation or an anion is considered dominant when it comprises more than 50 % of the total charge concentration. If no one cation and/or anion compose more than 50 % of the charge, then no facies are considered dominant. As shown in Tables 3-1 and 3-2, Ca^{2+} and HCO_3^- account for at least 50 % of the charge from cations and anions in the groundwater samples, respectively. Therefore the baseline Schoolcraft groundwater samples may be classified as calcium-bicarbonate.

3.9 Piper diagrams

One method of visually determining the facies classification of a water is by using a Piper diagram. Ion concentrations for a water sample are plotted on cation (Ca^{2+}, Mg^{2+}, Na^{+} and K^{+}) and anion (HCO_3^- and CO_3^{2-}, Cl^-, SO_4^{2-}) triangles and a central diamond-shaped diagram. The plotting locations on the diagram automatically determine whether any cation or anion is dominant. Two waters that have different total ion concentrations will be plotted on the same location on the diagram if the relative concentrations between the ions are similar. This allows quick comparison of water chemistry when two or more waters have very different ionic strengths.

One drawback of using conventional Piper diagrams for Schoolcraft groundwater is that NO_3^- is not included in the diagram. This omission is usually not a problem since most natural waters have small NO_3^- concentrations when compared to other anions like HCO_3^-, Cl^-, and SO_4^{2-}. However, if a water like the Schoolcraft Aquifer has a significant NO_3^- concentration (see Table 3-2), the anion facies derived from using a Piper diagram will be inaccurate. One solution to this problem is creating a modified Piper diagram that plots the concentration of NO_3^- with another anion (whichever has the smallest concentration).

As shown in Table 3-2, HCO_3^- and Cl^- have the highest percent of total anionic charge, 68.9 % and 15.7 %, respectively. Table 3-2 also shows that NO_3^- accounts for 8.8 % of the total anionic charge while SO_4^{2-} accounts for only 6.5 % of the total average anionic charge in the Schoolcraft baseline samples. In order to

include NO_3^- on a Piper diagram, all groundwater samples will be displayed on modified diagrams that combine nitrate with sulfate ($NO_3 + SO_4$) since SO_4^{2-} is present in the smallest concentration. Figure 3-2 is a modified Piper diagram for the baseline Schoolcraft groundwater samples.

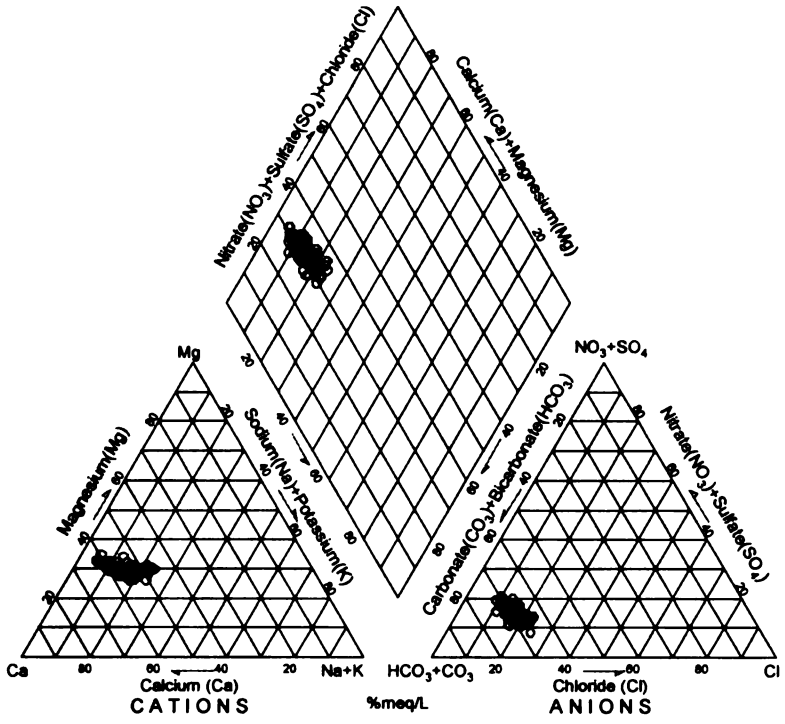

Figure 3-2. Modified Piper diagram of baseline groundwater samples

Figure 3-2 shows by the plotting position of baseline samples that groundwater from the Schoolcraft Aquifer may be classified as calcium-bicarbonate.

The composition of groundwater in the biotreatment zone will change as NaOH is injected into the subsurface to raise groundwater pH. The expected changes include increased Na^+ concentrations from the NaOH and decreased Ca^{2+}

and HCO_3^-, concentrations due to the expected precipitation of calcium carbonate minerals. It is expected that the groundwater will change from calcium-bicarbonate dominated to sodium-bicarbonate dominated. The geochemical changes that occur as groundwater in the biotreatment zone are discussed in Chapter 4.

CHAPTER 4

EFFLUENT CHEMISTRY OF 1-D COLUMNS

4.0 Introduction

As mentioned earlier, significant geochemical changes occur in the treatment zone as the pH of the groundwater is increased. A series of bench scale experiments was performed on Schoolcraft aquifer solids. Glass columns packed with Schoolcraft aquifer solids were flushed with groundwater that had been adjusted to pH 8.2. The ion concentration and pH of each column's effluent were monitored in order to determine the geochemical changes that occur as the solids were titrated. The flow through the columns represents a one-dimensional (1-D) titration of the solids that was used to represent and understand how the aquifer solids react during base addition.

4.1 Materials and methods

The following two sizes of Kontes® glass HPLC columns were to perform the solids titration experiments:

- Diameter: 1.5 centimeters (cm), Length: 15 cm, Volume: 24 mL, and
- Diameter: 1.5 cm, Length: 30 cm, Volume: 53 mL.

All columns were wet packed using aquifer solids collected from the biotreatment zone during the installation of the injection/extraction wells (see Figure 2-1). The sides of the columns were tapped periodically during filling to

enhance packing. Schoolcraft groundwater was then pumped through each column using a syringe pump until at least three pore volumes (as defined by a conservative tracer) of water had been exchanged or moved through the column.

Schoolcraft groundwater, adjusted to pH 8.2 using 1 M NaOH, was then pumped through each column and the effluent collected in 12-24 mL aliquots. Each aliquot was monitored for pH, alkalinity, major cations, major anions, and SiO_2, using the analytical methods discussed in Chapters 2 and 3.

The results of only one 1-D column experiment are discussed in this chapter. The impact on pH and ion concentrations in other columns is included in Appendix D. The relative response in terms of pH change and chemical makeup of the effluent was similar is all columns (see Appendix D).

4.2 Effluent pH

The pH of each effluent aliquot was measured immediately after collection in order to determine the number of pore exchanges required for pH breakthrough, or when effluent pH equals 95 % of the difference between the influent pH and original pH. Figure 4-1 shows the shape of a typical pH breakthrough curve for an experimental column packed with Schoolcraft aquifer solids.

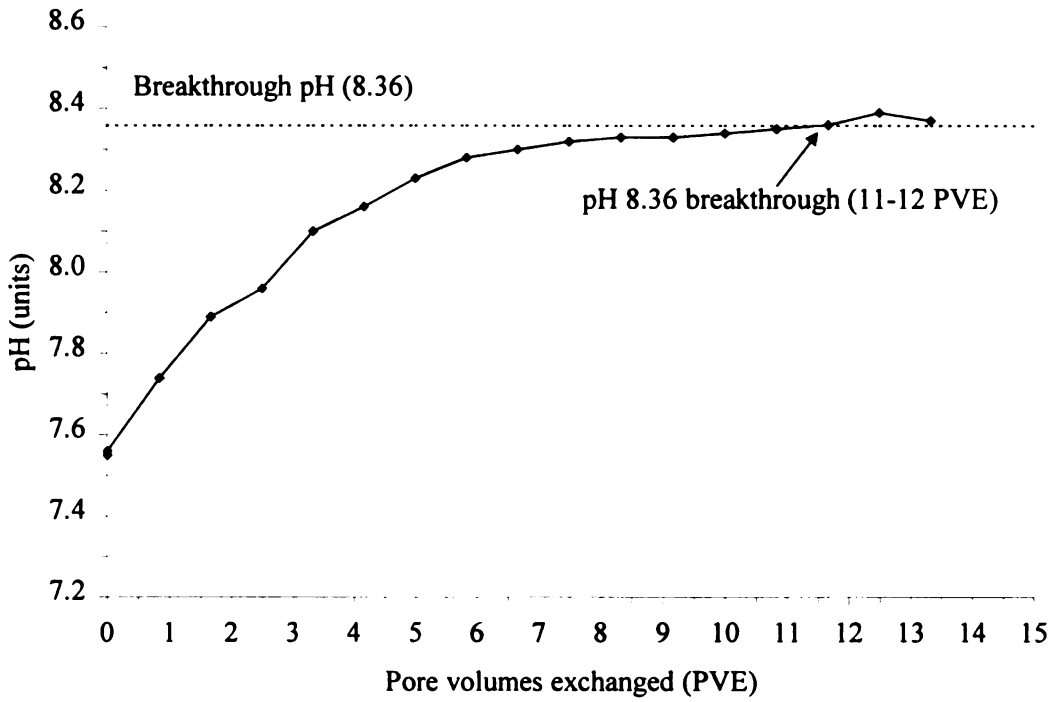

Figure 4-1. Typical pH breakthrough curve for an experimental column

Figure 4-1 illustrates that breakthrough at pH 8.36 occurred after about 11-12 pore exchanges.

4.3 Cation concentration in column effluent

The concentrations of major cations in the effluent of all 1-D columns were affected by pH as shown in Figure 4.2.

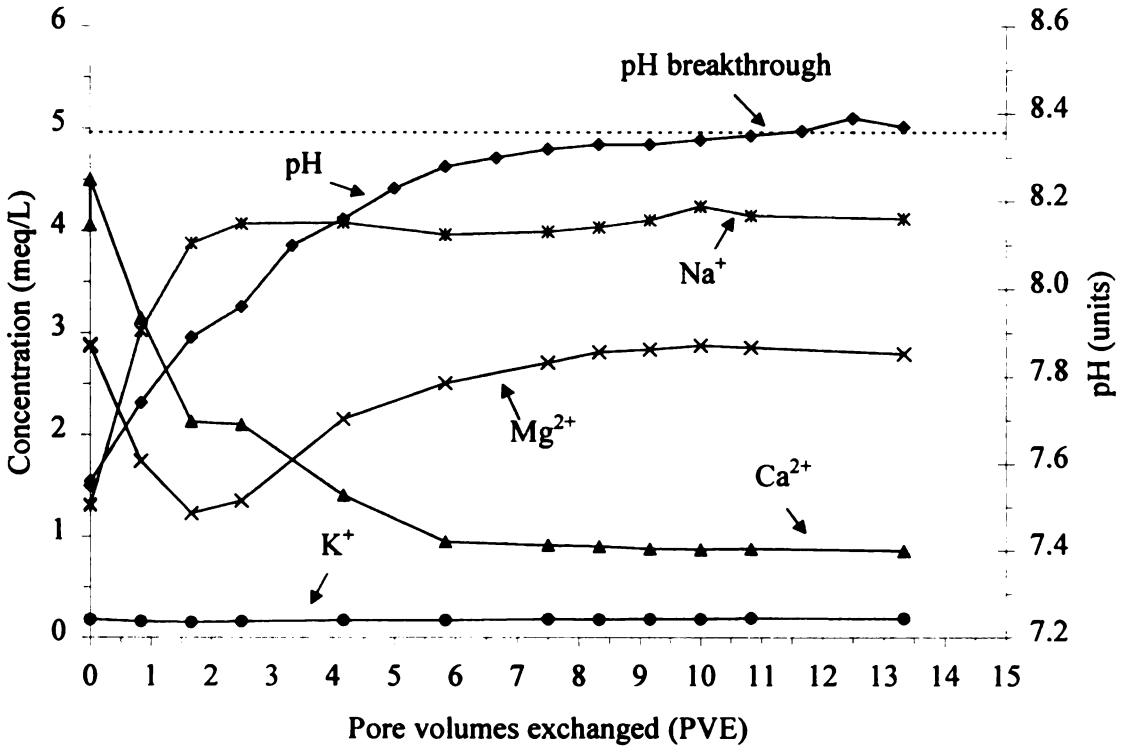

Figure 4-2. Major cations in effluent of a typical 1-D column

Figure 4-2 shows that the concentration of Na^+ increased with increasing pH. This increase in Na^+ concentration from 1.3 meq/L to 4.0 meq/L is due to the NaOH that was used to raise pH of the influent solution. Figure 4-2 shows that the concentration of Ca^{2+} decreased from 4.5 meq/L to 1 meq/L with increasing pH. The concentration of Mg^{2+} also decreased from 2.9 meq/L to 1.3 meq/L in the column effluent for about two pore exchanges before returning to its background concentration after about nine pore exchanges. There was less than 5 % change in the concentration of K^+ in the effluent during pH adjustment.

4.4 Anion concentration in column effluent

The anion concentration in the effluent of a typical 1-D column is shown in Figure 4-3.

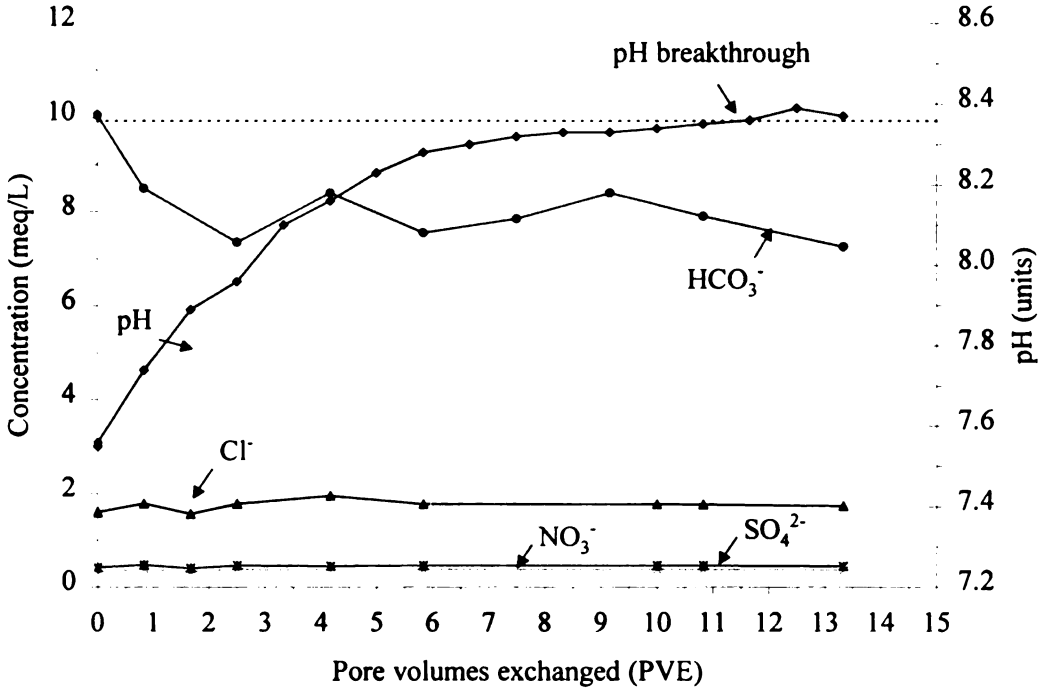

Figure 4-3. Major anions in effluent of a typical 1-D column

As shown in Figure 4-3, there were no significant changes in the concentrations of Cl^-, NO_3^- or SO_4^{2-} as pH increased in column effluent. However, as pH increased, effluent alkalinity (HCO_3^-) decreased below background concentrations. This decrease in HCO_3^- concentration is most likely due to the formation of carbonate minerals (see Chapter 5).

4.5 Piper diagram

The concentrations of ions in the 1-D column effluent were plotted using a modified Piper diagram (see Section 3.9). One advantage of using Piper diagrams, is that when two waters having very different chemistries are mixed in any proportion, the concentrations of the ions in the mixture will plot on a straight line between the two waters. The chemical composition of each effluent sample for Column B4 was plotted on a Piper diagram as shown in Figure 4-4.

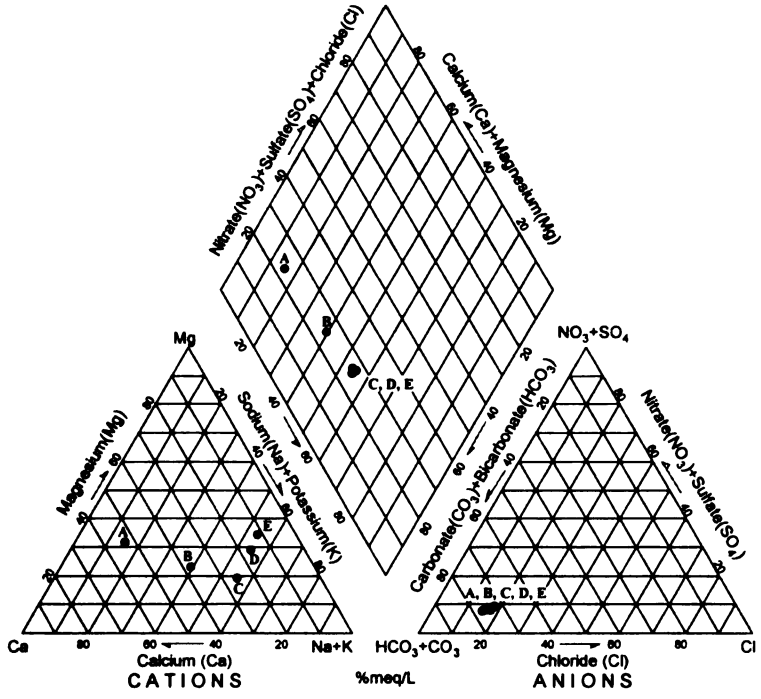

Figure 4-4. Modified Piper diagram showing 1-D column effluent

The points on the figure represent the effluent water chemistry from a 1-D column as the pH increases. Point A represents background water chemistry (see Figure

3-2) and point E represents pH-adjusted conditions. Figure 4-4 shows that from points A to C, the concentrations of Ca^{2+} and Mg^{2+} are both decreasing. These changes correspond to Region 1, where carbonate precipitation is occurring. From Points C to E, the concentration of Ca^{2+} is still decreasing, but the concentration of Mg^{2+} is increasing. Points C to E show the geochemical changes in Region 2 due to cation exchanged. The data from Figure 4-4, also shows that the water moves from being calcium-bicarbonate dominated (A) to sodium-bicarbonate dominated (C, D, E). The dramatic change in shape of a series of lines drawn through Points A through E suggests that two separate processes are controlling geochemical response as the pH increases. Points A through C may represents one process and Points C through E represent another. The two geochemical processes that control the concentration of cations in the effluent are discussed in Chapter 5.

CHAPTER 5

GEOCHEMICAL MECHANISMS

5.0 Introduction

The mechanisms that control geochemical changes that occur as base is added to the1-D columns (see Chapter 4) may predicted by evaluating the interaction between cations and anions and the surface of the aquifer solids. The precipitation of three carbonate minerals (aragonite, calcite, and dolomite) and cation exchange involving Ca^{2+} and Mg^{2+}, were evaluated.

5.1 Geochemical regions

Upon examining the shapes of the cation effluent curves for the 1-D column (see Figure 4-2), three regions that exhibited similar geochemical features were identified. These regions are shown on Figure 5-1.

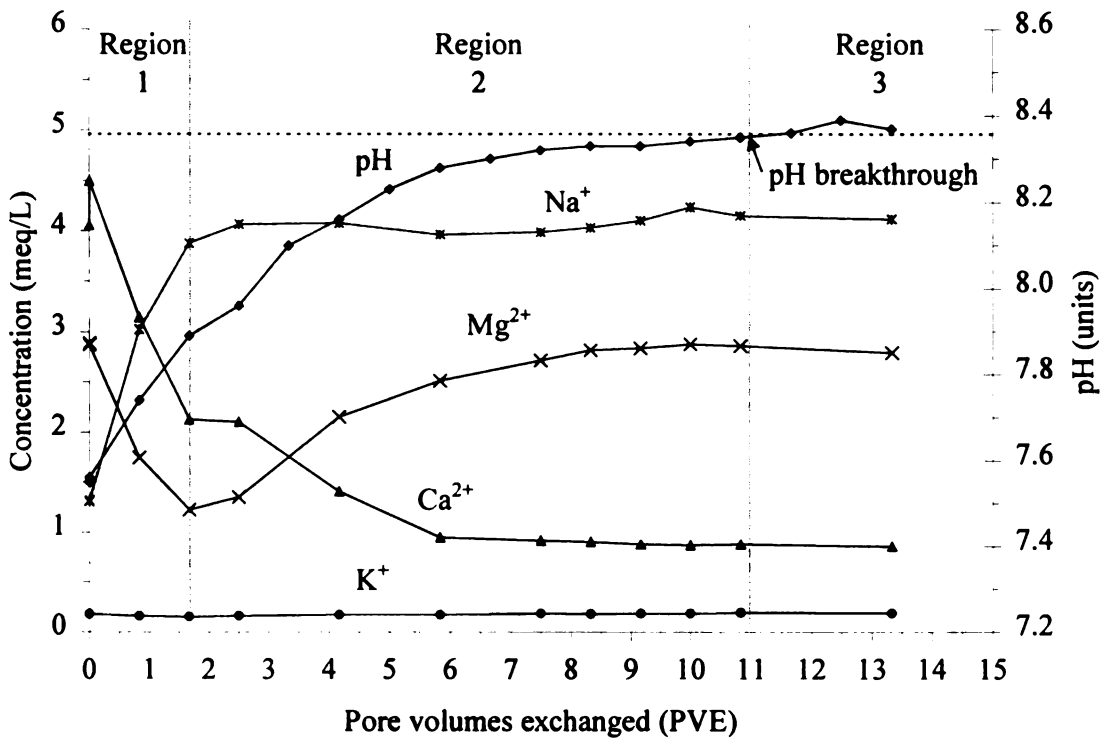

Figure 5-1. Geochemical regions in 1-D column effluent

As shown in Figure 5-1, the approximate ranges for the three regions are:

- Region 1: 0 to 1.5 pore volumes;
- Region 2: 1.5 to 11 pore volumes; and
- Region 3: 11 to 13 pore volumes.

5.1.1 Region 1

Figure 5-1 shows that the concentration of Na^+ reached its maximum effluent concentration of approximately 4 meq/L in Region 1. Na^+ acted similar to a conservative tracer during the 1-D experiments. The mixing or dispersion front that occurs as fluids travel through porous media has left the column in Region 1, since Na^+ has nearly reached its influent concentration. Since the dispersion front

had passed through the column at the end of Region 1, it is expected that any changes in water chemistry in Regions 2 and 3 are results of geochemical interactions and not dispersion. The concentrations of Ca^{2+} and Mg^{2+} decrease at approximately the same rate, which may suggest that, the geochemical processes affecting both of the cations may be related.

5.1.2 Region 2

Figure 5-1 shows that in Region 2, Na^{+} has reached its maximum concentration of 4 meq/L and the concentration of Ca^{2+} continues to decrease. Mg^{2+} reached a minimum concentration of 1.3 meq/L at approximately 1.5 pore volumes, but then began to increase again. The concentrations Ca^{2+} and Mg^{2+} throughout all of Region 2 are nearly mirror images of each other.

5.1.3 Region 3

Figure 5-1 shows that at approximately 11 pore volumes, pH breakthrough has finally occurred (see Chapter 4). The effluent pH and cation concentrations are approximately equal to influent conditions and the system is in a state of near equilibrium.

5.2 Carbonate formation

Carbonate minerals are the principle buffering mechanism in most natural waters. When alkali is added to a carbonate water system, Ca^{2+}, Mg^{2+}, and HCO_3^-

may combine to form calcium- and magnesium carbonates. As the solubility limits of these carbonates are exceeded, they may form minerals that precipitate out of solution. The three commonly occurring carbonate minerals are:

- Aragonite ($CaCO_3$),
- Calcite ($CaCO_3$), and
- Dolomite ($CaMg(CO_3)_2$).

The potential for each carbonate minerals to form in the 1-D column is discussed in the following sections.

5.2.1 Aragonite and calcite

Aragonite and calcite have the same molecular formula, $CaCO_3$, and are formed through similar processes. The presence and formation of calcite and aragonite are partially controlled by groundwater pH and the ratio of the concentration of Mg^{2+} with respect to Ca^{2+} (Mg^{2+}/Ca^{2+} ratio). High aqueous concentrations of Mg^{2+} inhibit the formation of calcite, but not aragonite (Drever, 1997). Therefore, waters with high Mg^{2+} concentrations (e.g., seawater) typically form aragonite and not calcite. In freshwaters (e.g., Schoolcraft groundwater), where the Mg^{2+}/Ca^{2+} ratio is low, calcite is typically the most abundant carbonate mineral (see Table 2-1). In order to determine which mineral was most likely to form in Schoolcraft groundwater, Figure 5-2 was developed to show the Mg^{2+}/Ca^{2+} ratio for the 1-D column effluent.

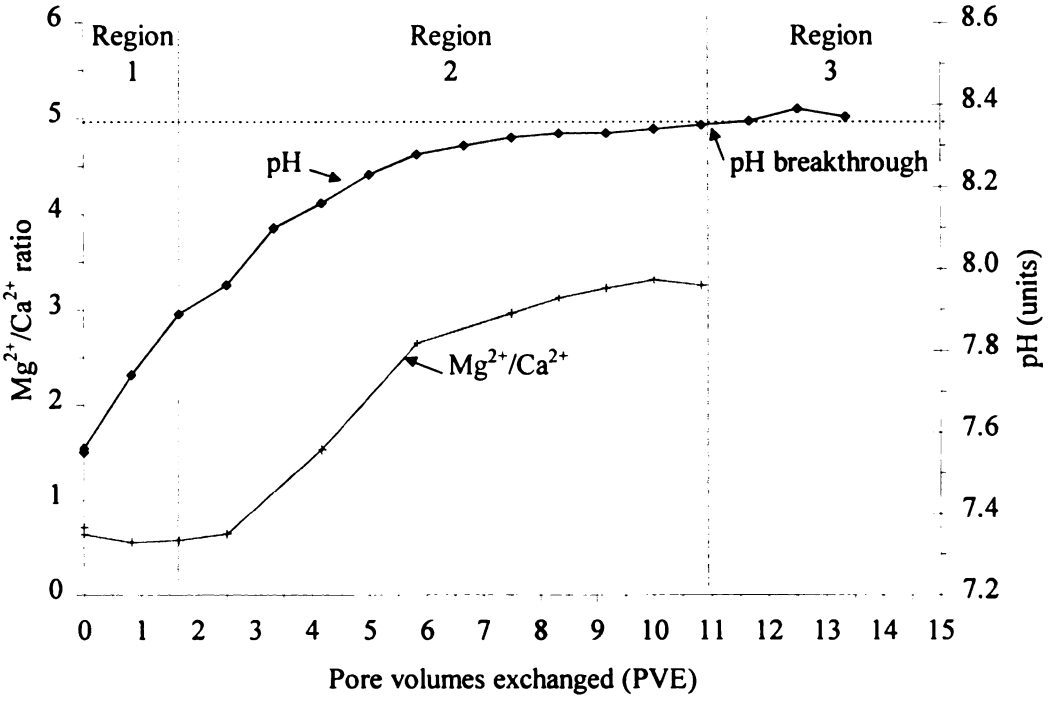

Figure 5-2. Mg^{2+}/Ca^{2+} ratio in 1-D column effluent

As shown in Figure 5-2, the Mg^{2+}/Ca^{2+} ratio in Region 1 is approximately 0.6. The Mg^{2+}/Ca^{2+} ratio remains constant during this period even through the concentrations both Mg^{2+} and Ca^{2+} are decreasing. The ratio remains constant since the concentrations of both cations are decreasing at the same rate (see Figures 4-2 and 5-1). The low Mg^{2+}/Ca^{2+} ratio of 0.6 calculated in Region 1, Mg^{2+} does not inhibit calcite precipitation (Drever, 1997), therefore calcite is more likely to form in the 1-D column than aragonite.

5.2.2 Dolomite

Dolomite is very unreactive at low temperatures (about 25 °C) and nearly impossible to form in the laboratory (Drever, 1997). Typically, dolomite forms only by the chemical alteration of an existing mineral like calcite or aragonite and not through direct precipitation. In addition, dolomite has much slower precipitation kinetics than calcite and aragonite and is therefore less likely to precipitate (Drever, 1997). Therefore, it is unlikely that the decrease in Ca^{2+}, Mg^{2+}, and HCO_3^- concentrations in Region 1 were due to the precipitation of dolomite.

5.2.3 Calcite precipitation

One way of determining if carbonate minerals are precipitating, is by examining the relative concentrations of Ca^{2+}, Mg^{2+}, and HCO_3^- as solution pH increases. Figure 5-3 shows the concentration of Ca^{2+}, Mg^{2+}, and HCO_3^- in the effluent of the 1-D column.

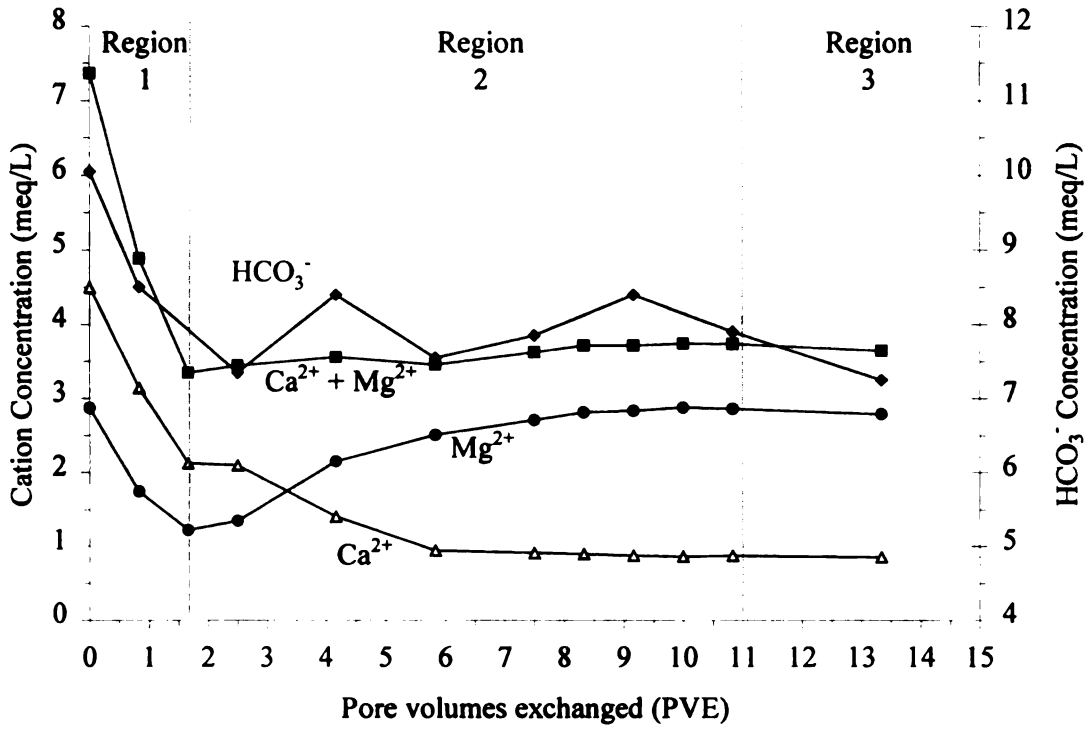

Figure 5-3. Concentrations of Ca^{2+}, Mg^{2+}, and HCO_3^- in 1-D column effluent

As shown on Figure 5-3, the concentrations of Ca^{2+} decreases at approximately the same rate as HCO_3^-. This stoichiometric decrease in the concentrations of Ca^{2+} and HCO_3^-, suggests that calcite is the lone carbonate mineral that precipitates as the pH increases in Region 1. The sawtooth-shaped variations in HCO_3^- concentration during Regions 2 and 3 are most likely due to measurement inaccuracies and therefore may not reflect the occurrence of other chemical processes. Equations describing this process are included in Tables A-2 and A-3 in Appendix A.

5.3 Cation exchange

The decrease in Mg^{2+} concentration observed in Region 1 cannot be described by the precipitation of carbonate minerals discussed in Section 5.2, therefore another geochemical process must be considered. Cation exchange can explain these changes in Mg^{2+} concentration in solution is due to cation exchange on the mineral surfaces. In Region 1, the concentration of Ca^{2+} decreases due to calcite precipitation (see Section 5.2).

During Region 2, the increase in the Mg^{2+}/Ca^{2+} ratio (see Figure 5-2) suggests that the cation exchange affinity for Mg^{2+} will increase, with respect to Ca^{2+}. This increased exchange affinity enables Mg^{2+} ions to replace Ca^{2+} ions present on the exchange complex. Figure 5-3 shows that this process actually occurs. During Region 2, the effluent concentration of Mg^{2+} remains lower than the influent concentration as Mg^{2+} ions leave solution and replace Ca^{2+} on the exchange complex. The effluent concentration of Mg^{2+} remains lower than the influent concentration until all available sites have been occupied by Mg^{2+} and the solution reaches equilibrium (Region 3). The concentration of Ca^{2+} during Region 2 is higher than the influent concentrations due to displaced Ca^{2+} ions leaving the cation exchange complex and therefore increasing the concentration of Ca^{2+} in solution. The effluent concentration of Ca^{2+} is higher than influent concentrations until all available Ca^{2+} sites have been occupied by Mg^{2+} and the solution reaches equilibrium (Region 3).

A simple depiction of how the composition of the base-exchange complex changes during the 1-D bench scale is included on Figure 5-4.

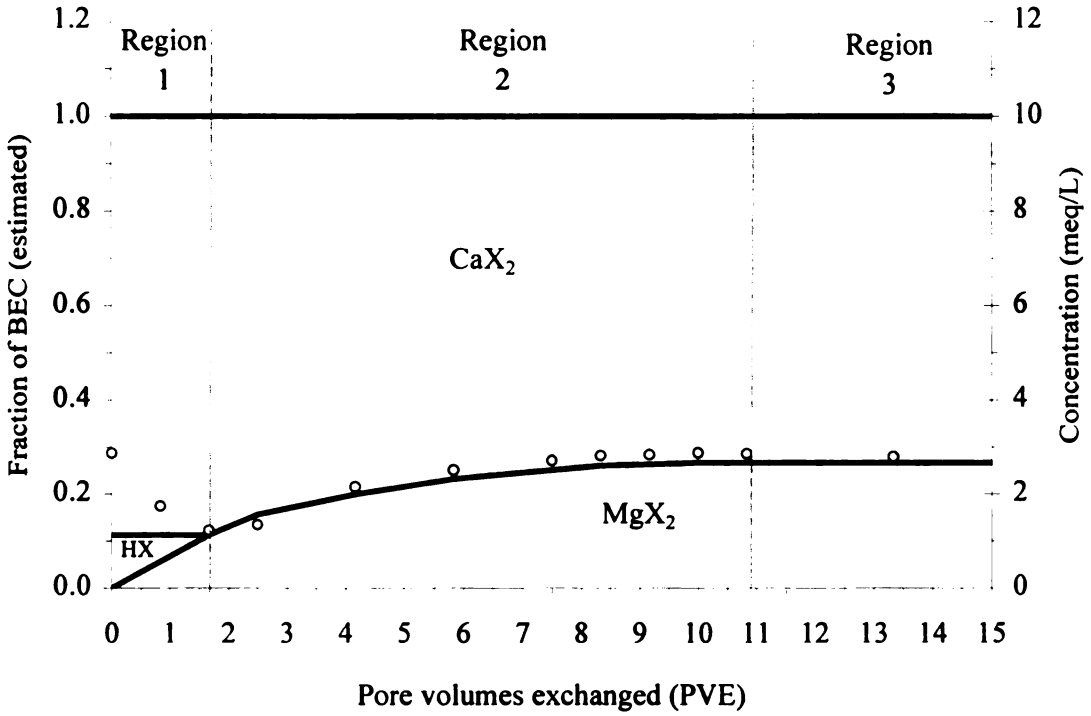

Figure 5-4. Estimated composition of base-exchange complex

The letter "X" in Figure 5-4 represents a cation exchange site on the mineral surface. Figure 5-4 illustrates that at zero pore volumes (Region 1), the base-exchange complex is composed of CaX_2 and HX. As alkali is added to the system, calcite begins to precipitate thus lowering the concentration of Ca^{2+} and HCO_3^- in the water. The hydrogen ions (H^+) associated with HCO_3^- and the base-exchange complex, begin to react with the OH^- provided by the alkali (NaOH). The Mg^{2+} ions in water then have a greater affinity for the HX sites begin to

displace the H^+ from the available sites on the solids. These displaced H^+ ion serve to buffer the water by neutralizing OH^-, and thus decrease the potential rate of pH adjustment. As shown on Figure 5-4, by the end of Region 1, Mg^{2+} has displaced H^+ from the available sites on the surface of the solids.

As the concentration of Ca^{2+} decreased in Region 1, the relative affinity for maintaining the CaX_2 sites also decreased. This lower affinity for base-exchange sites enables Mg^{2+} to displace Ca^{2+} from the CaX_2 sites on the aquifer solids. The shape of the lines in Table 5-3 illustrates this 1:1 stoichiometric replacement. As the concentration of Ca^{2+} decreased, the concentration of Mg^{2+} increased by the same magnitude. The influent concentrations of Ca^{2+} and Mg^{2+} are approximately 1 meq/L and 3 meq/L, respectively. The effluent concentration of Ca^{2+} is higher than the influent due to Ca^{2+} ions being displaced from the solids by Mg^{2+}. The effluent concentration of Mg^{2+} is lower than the influent concentration due to the Mg^{2+} ions leaving solution and occupying newly available sites on the base-exchange complex. The concentrations of Ca^{2+} and Mg^{2+} approach influent concentrations when Mg^{2+} has occupied all of the available CaX_2 sites. The physical changes that occur on the aquifer solids as a result of calcite precipitation and base cation exchange are discussed in Chapter 6.

It should be noted that Figure 5-4 is a simple depiction and it provides only general information that illustrates what happens to the base-exchange complex during pH adjustment. It is not meant to provide accurate values for BEC since the locations and shapes of the regions were empirically determined by comparing

effluent water chemistry with influent water chemistry. Differences in Mg^{2+} concentrations between the two were assumed to be due to Mg^{2+} exchange on the aquifer solids.

CHAPTER 6

IMPACT OF pH ADJUSTMENT ON AQUIFER SOLIDS

6.0 Introduction

The impact of pH adjustment on the aquifer solids was determined by comparing the properties of pH-adjusted samples (pH, base-exchange capacity and surface adsorption capacity) with a control and the characteristics of original core samples (Chapter 2).

6.1 Materials and methods

Experimental columns (Kontes®, Diameter: 1.5 cm, Length: 15 cm, Volume: 24 mL) were wet packed with aquifer solids from each core sample. Where practical, these columns were the same columns used in the 1-D column experiments. For each core sample, one column acted as a control and received only Schoolcraft groundwater (pH 7.4 ± 0.2), while the remaining column(s) received pH-adjusted groundwater (pH 8.3 ± 0.2). Initially, each column was flushed with Schoolcraft groundwater using a Harvard® syringe pump operating at a flow rate of 90 mL/hour. Flushing continued until three pore-volumes of water had been exchanged through each column or the effluent pH was constant.

Two hundred microliters (μL) of tritium (^3H) labeled water was injected at the inlet of each pH-adjusted column and two more pore volumes of water were flushed through the column. Tritium activity in 1-mL effluent aliquots was

measured in 10 mL of Safety-Solve® scintillation cocktail using a liquid scintillation counter. The porosity of each column was determined using the tritium concentration profile in the effluent samples. Porosity in the columns ranged from 35 % to 45 %, or pore volumes of 9 mL and 13 mL, respectively.

The pH-adjusted columns were then flushed with groundwater adjusted to pH 8.3 ± 0.2 using 1 M NaOH. The effluent was collected in 12-mL aliquots and immediately analyzed for pH. The composition and chemistry of these effluent samples is discussed in Chapter 4. The control columns were flushed with pH 7.4 groundwater until five additional pore water exchanges had occurred. No significant changes occurred in the effluent pH or chemistry of any of the control columns, indicating that any geochemical change in the pH-adjusted columns was a function of base addition and the resulting increase.

When the experiment was completed, the remaining water was forced out of the column using an air-filled syringe attached to the inlet of the column. The solids were then removed from the column, placed in an open plastic bag and allowed to air dry at room temperature for approximately one week. The impact of base addition (NaOH) on the aquifer solids was determined by comparing the properties of pH-adjusted solids sample with solids from the control column and the measurements from the original core samples (see Chapter 2).

6.2 Solids pH

The pH of the solids from the control and pH-adjusted columns was measured in order to determine solid pH changes that resulted from the column experiments and may be expected during field base addition. Selected solids pH values are included in Table 6-1.

Table 6-1. Solid pH values of pH-adjusted columns

Core Sample	Grain Texture	Cores pH (units)	Control Solids pH	pH-Adjusted Solids pH
D6-3111	Fine sand	9.03 ± 0.04	9.04 ± 0.05	9.08 ± 0.04
D4-7810	Medium sand	9.17 ± 0.05	9.08 ± 0.02	9.29 ± 0.02
D2-6608	Medium sand	9.17 ± 0.05	9.21 ± 0.04	9.40 ± 0.02

As shown in Table 6-1, there was no significant difference in the pH values for the core sample and the control column. However, the pH of the pH-adjusted medium sand is about 0.2 pH units higher than the control solids and thus statistically different from both the original core sample and control column. The higher pH of pH-adjusted solids suggests that composition and reactivity of solid surfaces was altered by pH adjustment and changes may be expected in total BEC and SAC.

6.3 Base exchangeable cations

Base-exchange capacity in soils typically increases with increasing pH (Pratt, 1961). As neutral exchange sites are converted to negatively charged sites

due to the increase concentration of OH^-. These newly available negatively charges site become available for cation exchange and thus increase the total BEC of the solids. However, to simplify the evaluation of the results, the total BEC of the solids was assumed to be constant. Table 6-2 contains selected information on the magnitude and composition of the base-exchange complex for Schoolcraft core samples, control solids and pH-adjusted solids.

Table 6-2. Base exchange composition of pH-adjusted solids

Cation	Cores (meq/100 g)	Control (meq/100 g)	pH-Adjusted (meq/100 g)
Ca^{2+}	3.44	1.24	1.51
Mg^{2+}	0.24	0.15	0.22
Na^+	Not measured	Not measured	Not measured
K^+	< 0.02	< 0.02	< 0.02

As Table 6-2 shows, the base exchange capacity of the aquifer cores for Ca^{2+} is over two times larger than the capacity for both the control and pH-adjusted solids. This difference in BEC is an artifact of column preparation as demonstrated by similar Ca^{2+} BEC for the control and pH-adjusted solids. When packing the columns (Chapter 4), the fine sand and clay particles tend to settle more slowly than larger particles. As a result, the larger grained solids tend to occupy most of the available space in the columns and smaller particles like clay minerals are excluded from the column. Clay-sized minerals typically have a higher surface

area per unit volume than sand-sized minerals. In addition, clay minerals may also participate in isomorphous substitution of ions in the structure of the clays. The substituted ions may increase the total BEC of a mineral.

Table 6-2 also shows that Mg^{2+} BEC is about 30% higher in the pH-adjusted solids (0.22 meq/100 g) than the control solids (0.15 meq/100g). As discussed in Section 5.3, the increased concentration on the exchange complex is due to Mg^{2+} occupying newly available sites due to Ca^{2+} displacement. The reported increase in Ca^{2+} BEC is not consistent with information obtained from water chemistry, therefore the dissolution of calcite during $SrCl_2$ displacement may have resulted in overestimating the amount of Ca^{2+} BEC on the solids. Similar BEC responses were also observed in other samples as shown in Table E-4 in Appendix E. However the total BEC for the control and pH-adjusted solids was also less than the BEC for the original core samples due to loss of fine-grained solids when packing the columns.

6.4 Carbonate content

Carbonate minerals like (calcite) are the primary pH buffers in the pH range that exists in the aquifer during groundwater pH-adjustment since both begin to precipitate at pH 8 (Drever, 1997). Carbonate precipitation helps control groundwater pH and concentration of Ca^{2+} and HCO_3^- during pH-adjustment. The total mass of carbonates that precipitate during pH-adjustment are negligible when compared to the total mass of carbonates in the solids (Schoolcraft Field

Bioaugmentation Experiment, 1997). Though immeasurable after, the concentration of calcite in the aquifer solids is expected to increase slightly due to mineral precipitation occurring in Region 1 (Chapters 4 and 5).

6.5 Surface adsorption capacity

The activity of surface adsorption sites for the core samples, control solids and pH-adjusted solids were measured using the NaF displacement method discussed in Chapter 2. The changes in surface complexing capacity on the surface of aquifer solids, before and after pH adjustment were not measurable using NaF.

CHAPTER 7

GEOCHEMICAL MODELING

7.0 Introduction

In order to validate explanations derived from the data collected from the 1-D column experiments, PHREEQC (Parkhurst, 1995), a geochemical equilibrium model was used to help describe the changes in the water chemistry. This model was used to predict the changes in pH and aqueous concentration of target components (Ca^{2+}, Mg^{2+} and HCO_3^-) as field groundwater pH-adjustment. The model may then be used as a tool to predict the response of another groundwater system subjected to similar remediation strategies based upon the solids composition and chemistry of the aquifer. The approach to quantify and model the impact of geochemical mechanisms may also be useful when predicting changes in groundwater chemistry during seawater intrusion.

7.1 Solid phase input parameters

PHREEQC allows users considerable flexibility when entering data into input files. The conceptual model consisted of a 1-D column containing solids with a porosity of 0.45. The magnitude of cation exchange capacity was defined for each cation based on measurements on the aquifer solids (Chapters 4 and 6) and is included in Table 7.1.

Table 7-1. Solid phase input parameters for PHREEQC data input file

Parameter	Actual	Modeled	Actual/Modeled
Porosity	0.45	0.45	1.0
Volume	53 cm^3	53 cm^3	1.0
Ca-exchange	0.0124	0.0124	1.0
Mg-exchange	0.0015	0.0015	1.0
Hfo_w	5.0E-6	0.0025	0.002

The magnitude of hydrous ferric oxides (Hfo) that are used to define surface complexing surfaces in the model helps control the number of pore volumes required for pH breakthrough (Chapter 4). The amount of hydrous ferric oxide was used as a calibration parameter to fit the simulated pH curve to the points generated during the experiment. Initially, Hfo was empirically determined by matching the shape of the modeled pH breakthrough curve with experimental data. For the 1-D column that was modeled in this experiment, a Hfo concentration that was 500 (1/0.002) times higher than the number of surface sites measured by NaF displacement (Chapter 2) was required for the modeled data to match the experimental results.

7.2 Liquid phase input parameters

The composition of at least two solutions must be defined when using the advective transport capabilities in PHREEQC. Solution "1" represents the groundwater chemistry at baseline conditions (pH 7.3-7.5) and solution "0"

represents pH-adjusted water that will be injected into the aquifer (pH 8.2-8.4). The chemical compositions of the waters used to define the solutions for the PHREEQC input file are shown in Table 7-2.

Table 7-2. Liquid phase input parameters for PHREEQC data input file

Parameter	Input Format	Pore Solution	Displacing Solution
Solution	Solution	1	0
pH (units)	pH	7.56	8.39
Temperature (°C)	Temp	25.0	25.0
Units	-units	ppm	ppm
Calcium	Ca	90.1	17.1
Magnesium	Mg	34.9	33.9
Sodium	Na	30.2	94.7
Potassium	K	7.0	7.3
Alkalinity	Alkalinity	613	442
Chloride	Cl	56.8	61.4
Nitrate	N(5)	20.1	22.8
Sulfate	S(6)	20.2	21.5
Silica	Si	14.2	13.5

The actual input file used in the simulations is included in Table F-1 in Appendix F. Chloride, nitrate, sulfate, and silica were not needed to simulate the geochemical changes in the 1-D column, but they were included to maintain charge balance.

As mentioned earlier, groundwater is continually trying to equilibrate with minerals that it is in contact with. However, in nearly all situations, the concentration of dissolved minerals are either undersaturated or supersatured with respect to equilibrium conditions. Saturation indices (SI) are one way to represent

the concentration conditions at a given pH, temperature and pressure. When log SI is greater than 0, the mineral is supersaturated and when log SI is less than 0, the mineral is undersaturated. The SI for selected minerals for the two solutions (before and after titration) are shown in Table 7-3.

Table 7-3. Saturation indices for effluent groundwater samples

Mineral	Pore Solution (log SI)	Displacing Solution (log SI)
pH (units)	7.56	8.3
Aragonite	-2.54	-3.71
Calcite	0.82	0.78
Dolomite	1.59	2.23
Quartz	0.35	0.32

Table showing SI for the minerals are included in Tables F-2 and F-3 in Appendix F. As shown in Table 7-3, both solutions are supersaturated with respect to calcite, dolomite and quartz. The log SI for calcite decreases as the pH of the water increases. As mentioned earlier (Chapters 4 and 5), carbonate minerals precipitate from solution as groundwater pH increases. This precipitation of carbonate minerals results in a lower concentration of minerals in solution and thus a lower log SI. Dolomite will not precipitate and therefore maintains a higher SI than calcite.

Table 7-3 also shows that the log SI for dolomite increased with increasing pH. Since the solution reaches saturation at lower concentrations at increasing pH, log SI for dolomite will increase, assuming the same mass of dolomite in solution.

Log SI for quartz remains fairly constant (0.35) for both baseline and pH-adjusted groundwater, suggesting that quartz and other silicate minerals do not undergo significant changes during base addition.

7.3 Simulated and experimental pH and cation concentrations

Experimental and simulated pH values and major cation concentrations for a 1-D column experiment are shown in Figure 7.1. Experimental data are shown as points, while solid lines represent simulated data.

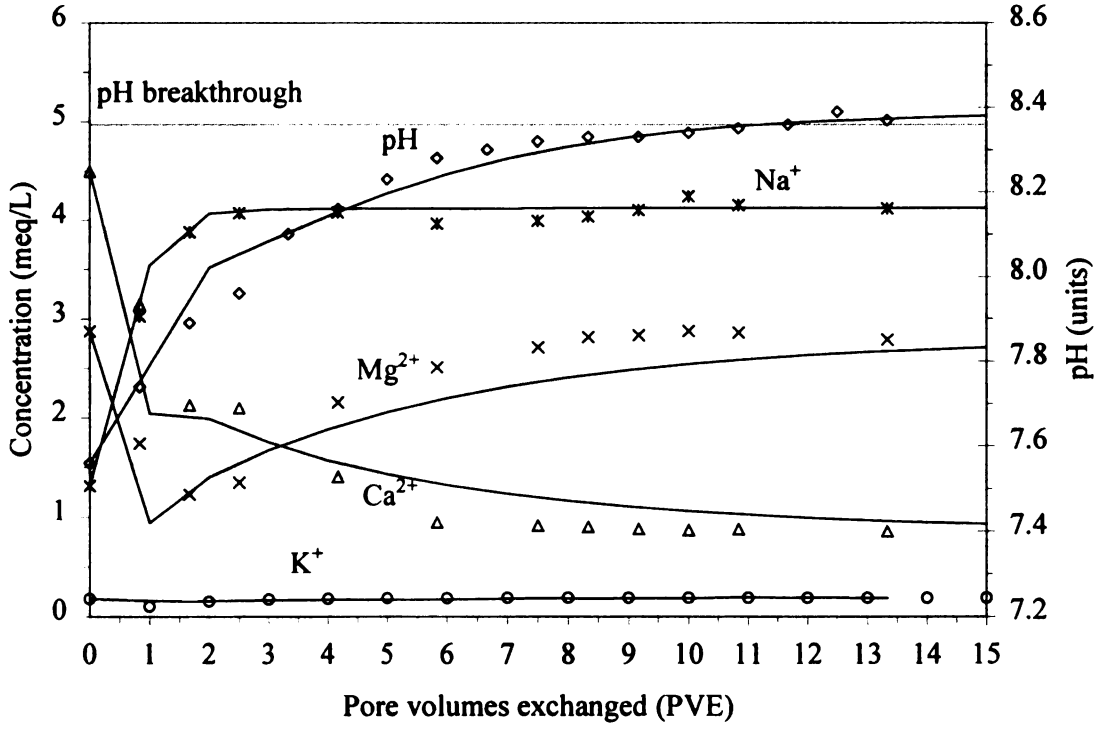

Figure 7-1. Experimental and simulated pH and concentrations of cations

As shown in Figure 7-1, the simulated values are very close to the measured pH and cation concentrations in the effluent of column B-4. The concentration of Na^+ and K^+ are also simulated well by this model. The simulation predicted pH values to within 0.1 pH units of the experimental data. The model predicted concentrations of Ca^{2+}, Mg^{2+}, Na^+, and K^+ to within, 0.4, 0.4, 0.2, and 0.1 meq/L, respectively.

The differences between experimental and simulated concentrations are most likely due to two reasons. One reason is the error associated with the analytical methods used to quantify the potential for involvement of cation exchange and surface complexation. The second and perhaps the most important difference stems from using a chemical equilibrium model to describe a system that has some kinetic response. In the PHREEQC model, mineral equilibria, cation exchange, and surface adsorption are all assumed to occur instantaneously, when in reality that is not the case. Each process takes time to occur. A model that incorporates kinetic parameters could be developed, but little information is available on the rates of most of the geochemical processes (NRC, 1990). In addition, the improved but small accuracy that may result from incorporating kinetic parameters is not justified when considering the additional time and expense required to develop such a model.

CHAPTER 8

SUMMARY AND APPLICATIONS

8.0 Summary

Mineral equilibria and cation exchange are important geochemical processes that control pH response as alkali is added to a solids and groundwater system (Chapter 1). The minerals that compose the solids portion of the system are primarily silicates and calcium carbonates (Chapter 2). Schoolcraft has an average pH of about 7.32 and is classified as calcium-bicarbonate (Chapter 3).

Calcite was the only major carbonate mineral observed to precipitate during pH-adjustment of the 1-D columns. Aragonite did not form during the experiment due to low Mg^{2+} concentrations and dolomite was prevented from precipitating by the environmental conditions and kinetic limitations. The precipitation of calcite resulted in an initial decrease in concentration of Ca^{2+} and HCO_3^- (Region 1). However the effluent concentration of Ca^{2+} remained above the influent concentrations until about 11 pore volumes (end of Region 2) of pH-adjusted water had passed through the 1-D columns (Chapters 4 and 5).

As the solution concentration of Ca^{2+} decreased, the Mg^{2+}/Ca^{2+} ratio increased. Mg^{2+} was then able to replace some of Ca^{2+} ions that occupied a portion of the cation exchange sites on the surface of the aquifer solids. Mg^{2+} ions left the displacing solution to occupy newly available exchange sites, resulting in the effluent concentration of Mg^{2+} being less than the influent concentration

during Regions 1 and 2. The Ca^{2+} ions displaced from the exchange sites by Mg^{2+} resulted in a Ca^{2+} effluent concentration that was higher than the influent concentration (Chapter 5).

The changes that occurred on the aquifer solids as a result of pH-adjustment indicated that the solids pH and BEC were both increased by base addition (Chapter 6). The geochemical impacts of pH-adjustment were simulated using mineral equilibria and cation exchange in the PHREEQC computer code. The PHREEQC simulation was able to effectively predict cation concentration to within 0.4 meq/L and pH to within 0.1 units.

8.1 Application

The results of this thesis indicate that cation exchange is an important process in even sandy soils, which are typically assumed to have very little geochemical reactivity. This thesis also provides a substantial source of site specific information on the:

- Equations that describe geochemical changes as a function of pH (Appendix A)
- Geochemical attributes of Schoolcraft Aquifer solids including solids pH (Chapter 2 and Appendix B)
- Geochemical attributes of Schoolcraft Aquifer solids including solids pH (Chapter 2 and Appendix B)
- Chemical makeup of Schoolcraft groundwater, including depth specific chemistry (Chapter 3 and Appendix C)

- Approach and methods that may be used to quantify geochemical changes that result from pH changes (Chapters 2 through 6)
- Changes that occur in groundwater chemistry as a result of pH adjustment (Chapter 4 and Appendix D)
- Impacts of pH-adjustment on aquifer solids (Chapter 6 and Appendix E)
- Application of the computer code PHREEQC for simulating geochemical data from bench-scale experiments (Chapter 7 and Appendix F)

In addition, the approach and results presented this thesis may be used to determine design and operation strategies for use in a full-scale field remediation project and simulate geochemical changes as a result of saltwater intrusion.

8.2 Recommendations for future work

Recommendations for future work include, but are not limited to, the following:

1. Determine geochemical impacts of long term base-adjustment
2. Simulate pH-adjustment in a 2-dimensional aquifer model.
3. Simulate pH-adjustment in a 3-dimensional full-scale remedial system.
4. Couple the geochemical predictions with a model that includes hydrogeology and microbiology to simulate hydraulic transport and microbial growth as a function of pH and ion concentration.
5. Examine the impact of pH-adjustment on the presence and availability of trace metals required for microbial growth.

APPENDICIES

APPENDIX A

APPENDIX A

EQUATIONS

Table A-1. General carbonate equilibrium equations

1. **Carbonic acid (H_2CO_3)**
   $H_2CO_3^* = CO_2(g) + H_2O$
   log K -1.468

2. **Bicarbonate (HCO_3^-)**
   $H_2CO_3 = H^+ + HCO_3^-$
   Log K -6.35

3. **Carbonate (CO_3^{2-})**
   $HCO_3^- = H^+ + CO_3^{2-}$
   log K -10.329

4. **Water (H_2O)**
   $H_2O = OH^- + H^+$
   log K -14.0

5. **pH**
   $pH = -\log[H^+]$

APPENDIX A

Table A-2. Selected carbonate equilibrium equations

1. **Calcium carbonate ($CaCO_3$)**
   $Ca^{2+} + CO_3^{2-} = CaCO_3$
   log K 3.224
   delta H 3.545 kcal

2. **Calcium bicarbonate ($CaHCO_3^+$)**
   $Ca^{2+} + HCO_3^- = CaHCO_3^+$
   log K 1.106
   delta H 2.69 kcal

3. **Magnesium carbonate ($MgCO_3$)**
   $Mg^{2+} + CO_3^{2-} = MgCO_3$
   log K 2.98
   delta H 2.713 kcal

4. **Magnesium bicarbonate ($MgHCO_3^+$)**
   $Mg^{2+} + HCO_3^- = MgHCO_3^+$
   log K 1.07
   delta H 0.79 kcal

5. **Sodium carbonate ($NaCO_3^-$)**
   $Na^+ + CO_3^{2-} = NaCO_3^-$
   log K 1.27
   delta H 8.91 kcal

6. **Sodium bicarbonate ($NaHCO_3$)**
   $Na^+ + HCO_3^- = NaHCO_3$
   log K -0.25

APPENDIX A

Table A-3. Selected mineral equilibrium equations

1. **Aragonite**
   $CaCO_3 = Ca^{2+} + CO_3^{2-}$
   log K -8.336

2. **Dolomite**
   $CaMg(CO_3)_2 = Ca^{2+} + Mg^{2+} + 2CO_3^{2-}$
   log K -16.54

3. **Calcite**
   $CaCO_3 = Ca^{2+} + CO_3^{2-}$
   log K -8.48

4. **Magnesite**
   $MgCO_3 = Mg^{2+} + CO_3^{2-}$
   log K -8.029

5. **Anhydrite**
   $CaSO_4 = Ca^{2+} + SO_4^{2-}$
   log K -4.36

6. **Gypsum**
   $CaSO4{:}2H_2O = Ca^{2+} + SO_4^{2-} + 2H_2O$
   log K -4.58

7. **Halite**
   $NaCl = Na^{+} + Cl^{-}$
   log K 1.582

8. **Quartz**
   $SiO_2 + 2H_2O = H_4SiO_4$
   log K -3.98

APPENDIX A

Table A-4. Selected cation exchange equations

1. **Calcium (CaX_2)**
   $Ca^{2+} + 2X^- = CaX_2$
   log K 0.8

2. **Magnesium (MgX_2)**
   $Mg^{2+} + 2X^- = MgX_2$
   log K 0.6

3. **Hydrogen (HX)**
   $H^+ + X^- = HX$
   log K 1.0

4. **Sodium (NaX)**
   $Na^+ + X^- = NaX$
   log K 0.0

5. **Potassium (KX)**
   $K^+ + X^- = KX$
   log K 0.7

APPENDIX A

Table A-5. Chemical surface adsorption equations

1. **Strong (Hfo_s)**
   a. $Hfo\_sOH + H^+ = Hfo\_s(OH)_2^+$
      log K 7.29 # = pKa1,int

   b. $Hfo\_sOH = Hfo\_sO^- + H^+$
      log K -8.93 # = -pKa2,int

2. **Weak (Hfo_w)**
   a. $Hfo\_wOH + H^+ = Hfo\_w(OH)_2^+$
      log K 7.29 # = pKa1,int

   b. $Hfo\_wOH = Hfo\_wO^- + H^+$
      log K -8.93 # = -pKa2,int

3. **Calcium**
   $Hfo\_sOH + Ca^{2+} = Hfo\_sOHCa^{2+}$
   log K 4.97

4. **Magnesium**
   $Hfo\_wOH + Mg^{2+} = Hfo\_wOMg^+ + H^+$
   log K -4.6

APPENDIX B

APPENDIX B

PROPERTIES OF SCHOOLCRAFT AQUIFER SOLIDS

Table B-1. Schoolcraft aquifer solids pH

Core ID	Well	Depth (ft bgs)	Type	pH in DDW	pH in $CaCl_2$
2-3000	2	30.00	Medium sand	9.02	Lost
2-3208	2	32.67	Silty sand	9.19	8.19
2-3508	2	35.67	Fine sand	9.12	8.18
2-4000	2	40.00	Fine sand	9.07	8.21
2-4600	2	46.00	Fine sand	9.22	8.32
2-4608	2	46.67	Fine sand	9.24	8.43
2-5107	2	51.58	Medium sand	9.26	8.26
2-5404	2	54.33	Medium sand	9.35	8.24
2-6010	2	60.83	Medium sand	9.43	8.05
2-6608	2	66.67	Medium sand	9.47	8.47
2-7201	2	72.08	Medium sand	9.34	8.35
2-7404	2	74.33	Medium sand	9.33	8.38
2-7606	2	76.50	Coarse sand	9.39	8.11
4-3200	4	32.00	Fine sand	9.29	8.26
4-3406	4	34.50	Fine sand	9.07	8.16
4-3610	4	36.83	Fine sand	9.18	8.20
4-4200	4	42.00	Medium sand	9.35	8.23
4-4500	4	45.00	Medium sand	9.13	8.27
4-4706	4	47.50	Medium sand	9.40	8.37
4-5200	4	52.00	Medium sand	9.40	8.31
4-5406	4	54.50	Coarse sand	9.14	Lost
4-6206	4	62.50	Medium sand	9.39	8.26
4-6604	4	66.33	Medium sand	9.06	8.24
4-7206	4	72.50	Coarse sand	9.25	8.17
4-7604	4	76.33	Coarse sand	9.43	8.27
4-7810	4	78.83	Coarse sand	9.48	8.30
6-3111	6	31.92	Fine sand	9.25	8.22
6-3406	6	34.50	Fine sand	9.16	8.30
6-3702	6	37.17	Fine sand	9.21	8.19
6-4102	6	41.17	Medium sand	9.07	8.10

Table B-1. (cont'd)

Core ID	Well	Depth (ft bgs)	Type	pH in DDW	pH in $CaCl_2$
6-4310	6	43.83	Medium sand	9.27	8.21
6-4604	6	46.33	Fine sand	9.09	8.20
6-5006	6	50.50	Medium sand	9.37	8.30
6-5302	6	53.17	Medium sand	9.24	8.30
6-5610	6	56.83	Coarse sand	8.46	7.89
6-5906	6	59.50	Coarse sand	9.27	8.30
6-6206	6	62.50	Medium sand	9.49	8.34
6-6500	6	65.00	Medium sand	9.42	8.25
6-6700	6	67.00	Fine sand	8.99	8.12
6-7206	6	72.50	Medium sand	9.51	8.24
6-8804	6	88.33	Coarse sand	-	-
8-3702	8	37.17	Fine sand	9.16	8.19
8-4104	8	41.33	Fine sand	9.13	8.12
8-4604	8	46.33	Medium sand	9.27	8.20
8-5010	8	50.83	Medium sand	9.36	8.29
8-5310	8	53.83	Medium sand	9.40	8.29
8-5610	8	56.83	Medium sand	9.48	8.22
8-6110	8	61.83	Medium sand	9.40	8.29
8-6508	8	65.67	Medium sand	9.17	8.11
8-7000	8	70.00	Coarse sand	9.42	8.32
8-7306	8	73.50	Coarse sand	9.35	8.14
8-7700	8	77.00	Coarse sand	9.31	8.06
8-8110	8	81.83	Coarse sand	-	-
8-8406	8	84.50	Coarse sand	-	-
10-3202	10	32.17	Fine sand	9.20	8.19
10-3511	10	35.92	Fine sand	9.34	8.09
10-3802	10	38.17	Fine sand	9.23	8.27
10-4206	10	42.50	Medium sand	9.34	8.10
10-4500	10	45.00	Fine sand	9.44	8.28
10-5008	10	50.67	Medium sand	9.41	8.30
10-5503	10	55.25	Medium sand	9.42	8.29
10-5802	10	58.17	Medium sand	9.49	8.35
10-6110	10	61.83	Medium sand	9.24	8.22
10-6406	10	64.50	Medium sand	9.41	8.29

APPENDIX B

Table B-1. (cont'd)

Core ID	Well	Depth (ft bgs)	Type	pH in DDW	pH in $CaCl_2$
10-6710	10	67.83	Fine sand	9.29	8.08
10-7106	10	71.50	Coarse sand	9.43	Lost
10-7610	10	76.83	Coarse sand	9.56	8.24
10-8500	10	85.00	Very coarse	-	-
14-3111	14	31.92	Fine sand	9.13	8.17
14-3406	14	34.50	Fine sand	9.33	8.27
14-3706	14	37.50	Fine sand	9.29	8.27
14-4104	14	41.33	Fine sand	9.30	8.20
14-5310	14	53.83	Medium sand	9.27	8.22
14-5908	14	59.67	Medium sand	9.47	8.33
14-6206	14	62.50	Medium sand	9.32	8.22
14-6610	14	66.83	Medium sand	9.38	8.30
14-7706	14	77.50	Coarse sand	9.46	8.32
14-8004	14	80.33	Medium sand	9.36	8.17
14-8303	14	83.25	Coarse sand	-	-
			Average	9.28 ± 0.16	8.23 ± 0.09
			No. Samples	74	71

APPENDIX B

Table B-2. Schoolcraft aquifer solid base exchange capacity

Core	Well	Depth (ft bgs)	Ca (meq/100 g)	Mg (meq/100 g)	K (meq/100 g)	Total (meq/100 g)
2-3000	2	30.00	0.70	0.13	< 0.02	0.85
2-3208	2	32.67	2.56	0.26	< 0.02	2.84
2-3508	2	35.67	3.60	0.29	< 0.02	3.91
2-4000	2	40.00	0.58	0.13	< 0.02	0.73
2-4600	2	46.00	3.37	0.27	< 0.02	3.65
2-4608	2	46.67	3.60	0.29	< 0.02	3.90
2-5107	2	51.58	3.05	0.28	< 0.02	3.33
2-5404	2	54.33	3.44	0.24	< 0.02	3.69
2-6010	2	60.83	2.95	0.22	< 0.02	3.17
2-6608	2	66.67	3.12	0.26	< 0.02	3.40
2-7201	2	72.08	2.81	0.25	< 0.02	3.07
2-7404	2	74.33	3.57	0.33	< 0.02	3.91
2-7606	2	76.50	3.44	0.25	< 0.02	3.70
4-3200	4	32.00	2.27	0.23	< 0.02	2.52
4-3406	4	34.50	3.21	0.35	0.03	3.58
4-3610	4	36.83	2.82	0.25	< 0.02	3.08
4-4200	4	42.00	4.68	0.29	< 0.02	4.99
4-4500	4	45.00	6.69	0.41	< 0.02	7.11
4-4706	4	47.50	3.16	0.24	< 0.02	3.42
4-5200	4	52.00	2.96	0.23	< 0.02	3.20
4-5406	4	54.50	3.16	0.23	< 0.02	3.39
4-6206	4	62.50	2.73	0.21	< 0.02	2.94
4-6604	4	66.33	3.15	0.32	< 0.02	3.47
4-7206	4	72.50	1.73	0.22	< 0.02	1.96
4-7604	4	76.33	2.64	0.24	< 0.02	2.88
4-7810	4	78.83	3.53	0.28	< 0.02	3.82
6-3111	6	31.92	0.85	0.16	< 0.02	1.03
6-3406	6	34.50	2.63	0.27	0.02	2.92
6-3702	6	37.17	0.89	0.19	< 0.02	1.10
6-4102	6	41.17	5.52	0.32	< 0.02	5.85
6-4310	6	43.83	6.01	0.34	< 0.02	6.36
6-4604	6	46.33	6.00	0.42	< 0.02	6.43
6-5006	6	50.50	2.81	0.24	< 0.02	3.05
6-5302	6	53.17	4.51	0.26	< 0.02	4.77

Table B-2. (cont'd)

Core ID	Well	Depth (ft bgs)	Ca (meq/100 g)	Mg (meq/100 g)	K (meq/100 g)	Total (meq/100 g)
6-5610	6	56.83	5.36	1.34	< 0.02	6.72
6-5906	6	59.50	4.09	0.29	< 0.02	4.39
6-6206	6	62.50	3.29	0.20	< 0.02	3.50
6-6500	6	65.00	2.43	0.17	< 0.02	2.62
6-6700	6	67.00	4.02	0.43	< 0.02	4.47
6-7206	6	72.50	3.23	0.23	< 0.02	3.46
6-8804	6	88.33	4.31	0.35	< 0.02	4.67
8-3702	8	37.17	2.16	0.25	< 0.02	2.42
8-4104	8	41.33	5.59	0.33	0.02	5.94
8-4604	8	46.33	3.88	0.34	< 0.02	4.23
8-5010	8	50.83	3.76	0.26	< 0.02	4.04
8-5310	8	53.83	3.68	0.23	< 0.02	3.93
8-5610	8	56.83	3.55	0.25	0.02	3.82
8-6110	8	61.83	3.80	0.28	< 0.02	4.09
8-6508	8	65.67	2.64	0.23	< 0.02	2.87
8-7000	8	70.00	3.59	0.29	< 0.02	3.88
8-7306	8	73.50	4.49	0.35	< 0.02	4.85
8-7700	8	77.00	4.44	0.28	< 0.02	4.73
8-8110	8	81.83	3.84	0.31	< 0.02	4.15
8-8406	8	84.50	3.51	0.41	< 0.02	3.93
10-3202	10	32.17	0.88	0.18	< 0.02	1.07
10-3511	10	35.92	3.78	0.25	< 0.02	4.05
10-3802	10	38.17	6.82	0.38	0.03	7.23
10-4206	10	42.50	3.42	0.27	< 0.02	3.70
10-4500	10	45.00	5.35	0.34	< 0.02	5.70
10-5008	10	50.67	3.89	0.23	< 0.02	4.13
10-5503	10	55.25	3.08	0.23	< 0.02	3.32
10-5802	10	58.17	3.01	0.25	< 0.02	3.27
10-6110	10	61.83	3.19	0.26	< 0.02	3.45
10-6406	10	64.50	3.45	0.26	< 0.02	3.71
10-6710	10	67.83	1.48	0.37	< 0.02	1.87
10-7106	10	71.50	5.19	0.42	< 0.02	5.62
10-7610	10	76.83	3.93	0.25	< 0.02	4.20
10-8500	10	85.00	3.59	0.39	< 0.02	3.99

Table B-2. (cont'd)

Core ID	Well	Depth (ft bgs)	Ca (meq/100 g)	Mg (meq/100 g)	K (meq/100 g)	Total (meq/100 g)
14-3111	14	31.92	1.95	0.23	< 0.02	2.20
14-3406	14	34.50	2.97	0.24	< 0.02	3.23
14-3706	14	37.50	4.50	0.33	0.02	4.85
14-4104	14	41.33	6.27	0.39	0.02	6.69
14-5310	14	53.83	4.53	0.26	< 0.02	4.80
14-5908	14	59.67	3.00	0.23	< 0.02	3.23
14-6206	14	62.50	4.16	0.26	< 0.02	4.42
14-6610	14	66.83	3.69	0.25	< 0.02	3.95
14-7706	14	77.50	3.41	0.22	< 0.02	3.63
14-8004	14	80.33	2.20	0.18	< 0.02	2.38
14-8303	14	83.25	2.27	0.26	< 0.02	2.55
		Average	3.47 ± 1.29	0.28 ± 0.13	< 0.02	3.77 ± 1.36
		No.	79	79	7 > MDL	79

APPENDIX C

APPENDIX C

SCHOOLCRAFT GROUNDWATER CHEMISTRY

Table C-1. Historical properties of Schoolcraft groundwater

Property (units)	Monitoring Wells Located Near Schoolcraft, Michigan[1]		
	Well 17[2]	Well 18[2]	Well 23[2]
Alkalinity (mg/L as CaCO3)	203	142	170
Arsenic (µg/L)	<1	<1	<1
Cadmium (µg/L)	<10	<10	<10
Calcium (mg/L)	69	83	70
Chloride (mg/L)	7.2	13	11
Chromium (µg/L)	<10	70	10
Copper (µg/L)	<10	<10	<10
Fluoride (mg/L)	0.1	0.4	0.2
Hardness (mg/L as CaCO3)	280	320	170
Iron (µg/L)	70	320	220
Lead (µg/L)	<100	<100	<100
Magnesium (mg/L)	27	28	23
Manganese (µg/L)	10	10	140
Nickel (µg/L)	<100	<100	<100
Nitrate (mg/L as N)	0.01	0.01	0.02
pH (units)	7.65	7.73	7.3
Phosphate (mg/L)	0.01	0.01	0.01
Potassium (mg/L)	0.4	0.6	0.7
Silica (mg/L)	9.8	11	7.6
Sodium (mg/L)	2.7	3.9	3.5
Specific Conductance (µS/cm)	572	730	582
Strontium (µg/L)	70	70	60
Sulfate (mg/L)	25	29	91
TDS-measured (mg/L)	282	418	308
Zinc (µg/L)	60	90	210

1 Geohydrology and Water Quality of Kalamazoo County, Michigan, 1986-88. U.S. Geological Survey. Water-Resources Investigations Report 90-4028.

2 Map showing location of wells is not included.

APPENDIX C

Table C-2. Contract laboratory analysis of Schoolcraft groundwater

Sample ID: MSU-MW34A
Collected by: M. Dybas
Collection date: March 17, 1997
Analysis method: ICP-AES
Analysis by: Contract Laboratory
Analysis date: March 28, 1997

Element	Symbol	Concentration (mg/L)
Aluminum	Al	< 0.050
Antimony	Sb	< 0.050
Arsenic	As	< 0.05
Barium	Ba	0.059
Boron	B	0.083
Cadmium	Cd	< 0.005
Calcium	Ca	107
Chromium	Cr	< 0.010
Cobalt	Co	< 0.005
Copper	Cu	< 0.005
Iron	Fe	< 0.010
Lead	Pb	0.009
Magnesium	Mg	33.1
Manganese	Mn	< 0.005
Mercury	Hg	< 0.100
Molybdenum	Mo	< 0.020
Nickel	Ni	< 0.01
Phosphorus	P	< 0.100
Potassium	K	6.80
Selenium	Se	0.100
Silicon	Si	6.63
Sodium	Na	35.2
Sulfur	S	8.16
Thallium	Tl	< 0.10
Vanadium	V	< 0.005
Zinc	Zn	0.018

APPENDIX C

Table C-3. Schoolcraft groundwater samples – May 09, 1997

Sample ID: MW34A (70 ft bgs)
Collected by: M. Dybas
Collection date: May 09, 1997
Analysis by: L. Warnick

Component	units	Valance	MW (mg/mmol)	Value	Charge (meq/L)	Mass (mg/L)
General						
Acidity	mg/L as $CaCO_3$	-	-	32.0	-	-
Alkalinity	mg/L as $CaCO_3$	-	-	383	-	-
Ph	units	-	-	7.3	-	-
Conductivity	umho	-	-	1,022	-	-
SiO_2	mg/L	-	60.1	13.5	-	13.5
				Total		13.5
Cations						
Ca^{2+}	mg/L	2	40.1	131	6.5	131
Mg^{2+}	mg/L	2	24.3	37.1	3.1	37.1
Na^{+}	mg/L	1	23.0	35.7	1.6	35.7
K^{+}	mg/L	1	39.1	5.5	0.1	5.5
				Total	11.3	209
Anions						
HCO_3^{-}	mg/L	1	61.0	468	7.7	230
Cl^{-}	mg/L	1	35.5	83.5	2.4	83.5
NO_3^{-}	mg/L	1	62.0	32.6	0.5	32.6
SO_4^{2-}	mg/L	2	96.1	27.1	0.6	27.1
				Total	11.1	373

Charge Balance (meq/L)

Total Cations	11.27
Total Anions	11.11
Cation/Anion	1.01

Solids Balance (mg/L)

Silica	13.50
Cations	209
Anions	373
TDS (calc)	596
TDS (meas)	555
Calculated/Measured	1.07

APPENDIX C

Table C-4. Schoolcraft groundwater samples – June 03, 1997

Collected by: M. Dybas
Collection date: June 03, 1997
Analysis by: L. Warnick

a. Filtered

Well	Sample[1]	Ca (mg/L)	K (mg/L)	Mg (mg/L)	Na (mg/L)	SiO_2 (mg/L)
MW34A	Stagnant #1	63.0	6.2	37.1	25.3	8.6
MW34A	Stagnant #2	63.3	6.5	37.5	24.6	8.6
MW34A	Purge 15 min #1	124.0	5.7	37.3	41.4	14.1
MW34A	Purge 15 min #2	124.9	5.2	36.3	40.6	13.7
MW34A	Purge 1.25 hr #1	117.8	5.4	36.7	37.0	13.9
MW34A	Purge 1.25 hr #2	89.6	5.4	37.4	35.6	14.0
EWS	Stagnant #1	72.0	23.4	1.7	2.1	12.9
EWS	Stagnant #2	70.9	23.6	2.0	2.3	12.8
EWS	Purge 40-L #1	92.1	29.2	13.0	4.5	12.6
EWS	Purge 40-L #2	94.3	29.3	13.0	4.7	12.8
EWS	Purge 100-L #1	96.7	28.5	12.6	4.5	12.5
EWS	Purge 100-L #2	96.5	30.0	12.6	4.8	12.9

b. Non-filtered

Well	Sample[1]	Ca (mg/L)	K (mg/L)	Mg (mg/L)	Na (mg/L)	SiO_2 (mg/L)
MW34A	Stagnant #1	62.9	6.2	36.0	23.9	8.3
MW34A	Stagnant #2	62.2	6.5	36.6	24.4	8.1
MW34A	Purge 15 min #1	124.0	6.1	37.2	40.8	13.9
MW34A	Purge 15 min #2	105.8	5.4	36.5	41.7	13.9
MW34A	Purge 1.25 hr #1	109.5	5.0	35.8	37.0	13.6
MW34A	Purge 1.25 hr #2	78.9	5.4	36.3	36.6	13.8
EWS	Stagnant #1	70.6	22.6	1.7	2.0	12.2
EWS	Stagnant #2	72.0	23.3	1.7	2.2	12.5
EWS	Purge 40-L #1	83.2	29.2	12.7	4.8	13.0
EWS	Purge 40-L #2	34.7	28.5	13.0	4.5	12.7
EWS	Purge 100-L #1	51.9	28.7	12.4	4.6	12.6
EWS	Purge 100-L #2	68.9	29.4	12.7	4.6	13.4

APPENDIX C

Table C-4. (cont'd)

a. Filtered

Well	Sample[1]	Al (mg/L)	Ba (mg/L)	Cd (mg/L)	Co (mg/L)	Cr (mg/L)	Cu (mg/L)
MW34A	03/27/1997[2]	< 0.04	0.241	< 0.004	< 0.007	< 0.007	< 0.006
MW34A	Stagnant #1	< 0.04	< 0.002	< 0.004	< 0.007	< 0.007	< 0.006
MW34A	Stagnant #2	< 0.04	< 0.002	< 0.004	< 0.007	< 0.007	< 0.006
MW34A	Purge 5 min #1	< 0.04	0.132	< 0.004	< 0.007	< 0.007	< 0.006
MW34A	Purge 5 min #2	< 0.04	0.131	< 0.004	< 0.007	< 0.007	< 0.006
MW34A	Purge 1.25 hr #1	< 0.04	0.116	< 0.004	< 0.007	< 0.007	< 0.006
MW34A	Purge 1.25 hr #2	< 0.04	0.116	< 0.004	< 0.007	< 0.007	< 0.006
EWS	Stagnant #1	< 0.04	< 0.002	< 0.004	< 0.007	< 0.007	< 0.006
EWS	Stagnant #2	< 0.04	< 0.002	< 0.004	< 0.007	< 0.007	< 0.006
EWS	Purge 40-L #1	0.944	< 0.002	< 0.004	< 0.007	< 0.007	< 0.006
EWS	Purge 40-L #2	0.975	< 0.002	< 0.004	< 0.007	< 0.007	< 0.006
EWS	Purge 100-L #1	0.340	< 0.002	< 0.004	< 0.007	< 0.007	< 0.006
EWS	Purge 100-L #2	0.659	< 0.002	< 0.004	< 0.007	< 0.007	< 0.006

b. Non-filtered

Well	Sample[1]	Al (mg/L)	Ba (mg/L)	Cd (mg/L)	Co (mg/L)	Cr (mg/L)	Cu (mg/L)
MW34A	Stagnant #1	< 0.04	< 0.002	< 0.004	< 0.007	< 0.007	< 0.006
MW34A	Stagnant #2	< 0.04	< 0.002	< 0.004	< 0.007	< 0.007	0.033
MW34A	Purge 5 min #1	< 0.04	0.136	< 0.004	< 0.007	< 0.007	< 0.006
MW34A	Purge 5 min #2	< 0.04	0.127	< 0.004	< 0.007	< 0.007	< 0.006
MW34A	Purge 1.25 hr #1	< 0.04	0.111	< 0.004	< 0.007	< 0.007	< 0.006
MW34A	Purge 1.25 hr #2	< 0.04	0.114	< 0.004	< 0.007	< 0.007	< 0.006
EWS	Stagnant #1	< 0.04	< 0.002	< 0.004	< 0.007	< 0.007	< 0.006
EWS	Stagnant #2	< 0.04	< 0.002	< 0.004	< 0.007	< 0.007	< 0.006
EWS	Purge 40-L #1	< 0.04	< 0.002	< 0.004	< 0.007	< 0.007	< 0.006
EWS	Purge 40-L #2	0.045	< 0.002	< 0.004	< 0.007	< 0.007	< 0.006
EWS	Purge 100-L #1	< 0.04	< 0.002	< 0.004	< 0.007	< 0.007	< 0.006
EWS	Purge 100-L #2	< 0.04	< 0.002	< 0.004	< 0.007	< 0.007	< 0.006

Table C-4. (cont'd)

a. Filtered

Well	Sample[1]	Fe (mg/L)	Mn (mg/L)	Ni (mg/L)	Pb (mg/L)	Sr (mg/L)	Zn (mg/L)
MW34A	03/27/1997[2]	0.040	< 0.002	< 0.015	< 0.04	0.161	0.650
MW34A	Stagnant #1	< 0.007	< 0.002	< 0.015	< 0.04	0.052	1.131
MW34A	Stagnant #2	< 0.007	< 0.002	< 0.015	< 0.04	0.051	1.107
MW34A	Purge 5 min #1	< 0.007	< 0.002	< 0.015	< 0.04	0.141	0.134
MW34A	Purge 5 min #2	< 0.007	< 0.002	< 0.015	< 0.04	0.141	0.135
MW34A	Purge 1.25 hr #1	< 0.007	< 0.002	< 0.015	< 0.04	0.139	0.060
MW34A	Purge 1.25 hr #2	< 0.007	< 0.002	< 0.015	< 0.04	0.143	0.050
EWS	Stagnant #1	< 0.007	< 0.002	< 0.015	< 0.04	0.151	< 0.002
EWS	Stagnant #2	< 0.007	< 0.002	< 0.015	< 0.04	0.150	< 0.002
EWS	Purge 40-L #1	1.130	0.019	< 0.015	< 0.04	0.163	< 0.002
EWS	Purge 40-L #2	1.204	0.018	< 0.015	< 0.04	0.164	< 0.002
EWS	Purge 100-L #1	0.502	0.010	< 0.015	< 0.04	0.164	< 0.002
EWS	Purge 100-L #2	0.802	0.019	< 0.015	0.122	0.164	< 0.002

b. Non-filtered

Well	Sample[1]	Fe (mg/L)	Mn (mg/L)	Ni (mg/L)	Pb (mg/L)	Sr (mg/L)	Zn (mg/L)
MW34A	Stagnant #1	< 0.007	< 0.002	< 0.015	< 0.04	0.052	1.202
MW34A	Stagnant #2	0.021	< 0.002	< 0.015	< 0.04	0.054	1.668
MW34A	Purge 5 min #1	< 0.007	< 0.002	< 0.015	< 0.04	0.141	0.285
MW34A	Purge 5 min #2	< 0.007	< 0.002	< 0.015	< 0.04	0.141	0.162
MW34A	Purge 1.25 hr #1	< 0.007	< 0.002	< 0.015	< 0.04	0.140	0.066
MW34A	Purge 1.25 hr #2	< 0.007	< 0.002	< 0.015	< 0.04	0.141	0.047
EWS	Stagnant #1	< 0.007	< 0.002	< 0.015	0.080	0.151	< 0.002
EWS	Stagnant #2	< 0.007	< 0.002	< 0.015	< 0.04	0.151	< 0.002
EWS	Purge 40-L #1	< 0.007	< 0.002	< 0.015	< 0.04	0.162	< 0.002
EWS	Purge 40-L #2	< 0.007	< 0.002	< 0.015	0.495	0.165	< 0.002
EWS	Purge 100-L #1	< 0.007	< 0.002	< 0.015	< 0.04	0.165	< 0.002
EWS	Purge 100-L #2	< 0.007	< 0.002	< 0.015	< 0.04	0.165	< 0.002

1 Stagnant samples were collected to evaluate potential for trace metal contamination.

2 Sample collected on March 27, 1997.

APPENDIX C

Table C-5. Schoolcraft groundwater samples – July 02, 1997

Collected by: M. Dybas
Collection date: July 02-03, 1997
Analysis by: L. Warnick
Analysis date: July 07, 1997

Sample	Depth	Collection Date	pH (units)	Acidity (meq/L)	Alkalinity (meq/L)	SiO_2 (mmol/L)
SB-A-30.1	30	07/02/1997	7.47	0.43	7.22	0.25
SB-A-30.2	30	07/02/1997	7.70	0.56	6.92	0.27
SB-A-30.3	30	07/02/1997	7.48	0.56	7.16	0.27
SB-A-40	40	07/02/1997	7.60	0.59	7.42	0.26
SB-A-50	50	07/02/1997	7.54	0.61	7.04	0.25
SB-A-60	60	07/02/1997	7.48	0.62	6.54	0.26
SB-A-70.1	70	07/02/1997	7.58	0.51	6.16	0.25
SB-A-70.2	70	07/02/1997	7.57	0.50	6.16	0.25
SB-A-70.3	70	07/02/1997	7.64	0.45	6.26	0.29
SB-A-80	80	07/02/1997	7.52	0.58	6.46	0.27
SB-B-40	40	07/03/1997	7.41	0.84	6.54	0.23
SB-B-50	50	07/03/1997	7.33	0.74	7.14	0.29
SB-B-60	60	07/03/1997	7.30	0.87	8.02	0.29
SB-B-70.1	70	07/03/1997	7.25	0.82	7.36	0.25
SB-B-70.2	70	07/03/1997	7.17	0.90	7.30	0.25
SB-B-70.3	70	07/03/1997	7.27	0.77	7.56	0.29
SB-B-80	80	07/03/1997	7.24	0.82	7.42	0.30
SB-B-90	90	07/03/1997	7.18	0.94	7.30	0.25

Table C-5. (cont'd)

Sample	Ca (meq/L)	Mg (meq/L)	Na (meq/L)	K (meq/L)	Cations Total
SB-A-30.1	5.72	2.63	1.43	0.26	10.13
SB-A-30.2	5.78	2.66	1.42	0.20	10.23
SB-A-30.3	5.74	2.66	1.46	0.18	10.20
SB-A-40	5.62	2.69	1.48	0.17	10.08
SB-A-50	5.73	2.98	1.29	0.17	10.22
SB-A-60	6.14	3.12	0.76	0.08	10.17
SB-A-70.1	5.41	2.78	0.56	0.07	8.84
SB-A-70.2	5.37	2.76	0.56	0.08	8.85
SB-A-70.3	5.37	2.82	0.57	0.07	8.92
SB-A-80	5.81	3.17	0.61	0.04	9.67
SB-B-40	5.21	2.85	1.13	0.17	9.51
SB-B-50	5.68	3.05	1.05	0.15	10.09
SB-B-60	6.47	3.26	0.91	0.22	11.05
SB-B-70.1	6.13	3.18	0.84	0.19	10.38
SB-B-70.2	6.14	3.18	0.86	0.18	10.40
SB-B-70.3	6.16	3.24	0.86	0.19	10.57
SB-B-80	6.52	3.46	0.97	0.11	11.12
SB-B-90	6.41	3.57	1.17	0.08	11.37

Table C-5. (cont'd)

Sample	HCO_3 (meq/L)	Cl (meq/L)	NO_3 (meq/L)	SO_4 (meq/L)	Anions Total	Cations/ Anions
SB-A-30.1	7.22	2.07	0.68	0.49	10.47	0.97
SB-A-30.2	6.92	2.10	0.68	0.51	10.21	1.00
SB-A-30.3	7.16	2.10	0.68	0.50	10.44	0.98
SB-A-40	7.42	1.97	0.58	0.53	10.50	0.96
SB-A-50	7.04	1.91	0.73	0.59	10.27	1.00
SB-A-60	6.54	1.92	0.84	0.60	9.91	1.03
SB-A-70.1	6.16	0.93	0.74	0.73	8.56	1.03
SB-A-70.2	6.16	0.93	0.74	0.75	8.58	1.03
SB-A-70.3	6.26	0.94	0.75	0.77	8.72	1.02
SB-A-80	6.46	1.14	0.95	0.78	9.33	1.04
SB-B-40	6.54	1.43	0.99	0.62	9.58	0.99
SB-B-50	7.14	1.34	1.03	0.70	10.21	0.99
SB-B-60	8.02	1.30	1.05	0.64	11.01	1.00
SB-B-70.1	7.36	1.10	1.16	0.70	10.32	1.01
SB-B-70.2	7.30	1.11	1.17	0.70	10.28	1.01
SB-B-70.3	7.56	1.14	1.15	0.69	10.53	1.00
SB-B-80	7.42	1.13	1.53	0.65	10.73	1.04
SB-B-90	7.30	1.88	0.14	1.71	11.03	1.03

APPENDIX C

Table C-6. Baseline Schoolcraft groundwater – September 19, 1997

Collected by: M. Dybas
Collection date: September 19, 1997
Analysis by: L. Warnick

Sample ID	Well	Depth	Collection Date	pH (units)	SiO_2 (mg/L)
M5.45.1M	M5	45	09/19/97	7.486	12.6
M5.55.1M	M5	55	09/19/97	7.325	13.5
M5.65.1M	M5	65	09/19/97	7.337	13.1
M5.75.1M	M5	75	09/19/97	7.298	13.0
M6.45.1M	M6	45	09/19/97	7.351	11.7
M6.55.1M	M6	55	09/19/97	7.344	12.5
M6.65.1M	M6	65	09/19/97	7.342	13.2
M6.75.1M	M6	75	09/19/97	7.284	13.4
M7.45.1M	M7	45	09/19/97	7.311	12.3
M7.55.1M	M7	55	09/19/97	7.346	12.6
M7.65.1M	M7	65	09/19/97	7.321	12.8
M7.75.1M	M7	75	09/19/97	7.325	13.2
M8.45.1M	M8	45	09/19/97	7.279	13.7
M8.55.1M	M8	55	09/19/97	7.344	12.5
M8.65.1M	M8	65	09/19/97	7.318	13.1
M8.75.1M	M8	75	09/19/97	7.376	13.8
M9.45.1M	M9	45	09/19/97	7.314	11.6
M9.55.1M	M9	55	09/19/97	7.412	11.3
M9.65.1M	M9	65	09/19/97	7.318	13.4
M9.75.1M	M9	75	09/19/97	7.321	15.6
M10.45.1M	M10	45	09/19/97	7.318	13.0
M10.55.1M	M10	55	09/19/97	7.316	10.3
M10.65.1M	M10	65	09/19/97	7.328	12.8
M10.75.1M	M10	75	09/19/97	7.323	10.7
M11.45.1M	M11	45	09/19/97	7.353	12.8
M11.55.1M	M11	55	09/19/97	7.359	12.6
M11.65.1M	M11	65	09/19/97	7.341	12.5
M11.75.1M	M11	75	09/19/97	7.346	12.8
M12.45.1M	M12	45	09/19/97	7.347	11.9
M12.55.1M	M12	55	09/19/97	7.339	12.6
M12.65.1M	M12	65	09/19/97	7.319	13.2
M12.75.1M	M12	75	09/19/97	7.330	14.1

Table C-6. (cont'd)

Sample ID	Ca (mg/L)	Mg (mg/L)	Na (mg/L)	K (mg/L)
M5.45.1M	89.5	30.8	31.7	5.6
M5.55.1M	96.4	29.7	30.7	5.8
M5.65.1M	96.2	30.1	37.7	5.9
M5.75.1M	108.2	32.1	31.2	4.7
M6.45.1M	80.9	31.8	41.8	3.4
M6.55.1M	96.7	29.6	25.1	5.8
M6.65.1M	106.4	31.0	35.6	4.0
M6.75.1M	117.7	34.9	22.5	2.7
M7.45.1M	89.9	31.0	28.4	6.1
M7.55.1M	95.9	29.7	21.8	4.3
M7.65.1M	101.1	28.8	36.2	3.5
M7.75.1M	99.2	30.3	32.1	4.0
M8.45.1M	91.1	30.4	23.9	7.2
M8.55.1M	96.1	28.7	21.7	4.7
M8.65.1M	98.3	30.1	28.5	4.8
M8.75.1M	87.6	28.3	12.4	2.2
M9.45.1M	74.6	29.5	38.8	4.0
M9.55.1M	78.2	27.3	39.6	4.3
M9.65.1M	104.7	31.7	35.7	5.4
M9.75.1M	109.5	32.4	24.6	3.0
M10.45.1M	99.1	30.1	22.3	4.4
M10.55.1M	66.1	24.8	28.6	5.0
M10.65.1M	99.5	29.0	34.0	3.5
M10.75.1M	72.7	25.9	36.2	< 0.638
M11.45.1M	92.8	30.6	19.3	5.6
M11.55.1M	94.4	29.5	16.1	3.9
M11.65.1M	93.5	29.3	15.9	3.4
M11.75.1M	90.9	28.9	14.0	3.5
M12.45.1M	85.3	31.3	29.5	5.2
M12.55.1M	95.8	28.8	25.3	5.1
M12.65.1M	103.4	30.6	29.1	3.6
M12.75.1M	105.3	34.0	26.2	1.0

Table C-6. (cont'd)

Sample ID	HCO_3 (mg/L)	Cl (mg/L)	NO_3 (mg/L)	SO_4 (mg/L)
M5.45.1M	412	74.1	53.8	29.5
M5.55.1M	427	65.3	56.0	29.1
M5.65.1M	445	77.6	50.6	28.6
M5.75.1M	447	83.5	42.3	27.9
M6.45.1M	387	80.0	47.1	29.1
M6.55.1M	435	50.1	52.5	28.6
M6.65.1M	462	87.7	47.4	28.4
M6.75.1M	465	76.2	47.1	28.6
M7.45.1M	410	56.8	57.7	27.5
M7.55.1M	416	45.0	61.1	29.0
M7.65.1M	442	60.6	57.6	28.6
M7.75.1M	436	59.2	55.2	27.3
M8.45.1M	412	61.1	49.5	26.0
M8.55.1M	403	55.5	37.5	28.6
M8.65.1M	424	61.9	48.2	27.1
M8.75.1M	372	43.6	54.1	33.8
M9.45.1M	395	77.2	42.5	31.0
M9.55.1M	419	69.7	48.4	25.6
M9.65.1M	450	81.5	46.8	29.4
M9.75.1M	387	38.7	63.1	31.1
M10.45.1M	416	42.7	71.1	28.3
M10.55.1M	400	48.9	64.3	29.0
M10.65.1M	441	65.8	56.9	29.0
M10.75.1M	447	58.1	56.8	32.0
M11.45.1M	397	57.1	50.7	29.5
M11.55.1M	387	48.2	37.9	30.1
M11.65.1M	395	40.4	59.1	30.0
M11.75.1M	380	41.5	55.0	32.3
M12.45.1M	392	61.5	57.7	28.8
M12.55.1M	424	51.7	65.4	28.0
M12.65.1M	439	71.7	51.0	30.2
M12.75.1M	421	59.2	62.8	29.7

APPENDIX C

Table C-6. (cont'd)

Sample ID	Al (mg/L)	Ba (mg/L)	Cu (mg/L)	Fe (mg/L)	Mn (mg/L)
M5.45.1M	0.215	0.05	< 0.031	< 0.058	< 0.015
M5.55.1M	0.183	0.047	< 0.031	< 0.058	< 0.015
M5.65.1M	0.167	0.052	< 0.031	< 0.058	< 0.015
M5.75.1M	0.224	0.053	< 0.031	< 0.058	< 0.015
M6.45.1M	0.0709	0.0641	< 0.031	0.1262	0.0392
M6.55.1M	0.179	0.042	< 0.031	< 0.058	< 0.015
M6.65.1M	0.192	0.048	< 0.031	< 0.058	< 0.015
M6.75.1M	0.0263	0.043	< 0.031	< 0.058	0.036
M7.45.1M	0.216	0.044	< 0.031	< 0.058	< 0.015
M7.55.1M	0.204	0.043	< 0.031	< 0.058	< 0.015
M7.65.1M	0.194	< 0.008	< 0.031	< 0.058	< 0.015
M7.75.1M	0.216	0.05	< 0.031	< 0.058	< 0.015
M8.45.1M	0.171	0.048	< 0.031	< 0.058	< 0.015
M8.55.1M	0.2	0.043	< 0.031	< 0.058	< 0.015
M8.65.1M	0.185	0.048	< 0.031	< 0.058	< 0.015
M8.75.1M	0.147	0.033	< 0.031	< 0.058	< 0.015
M9.45.1M	0.0259	0.0634	< 0.031	< 0.058	< 0.015
M9.55.1M	< 0.006	0.0597	< 0.031	< 0.058	0.0323
M9.65.1M	0.196	0.057	< 0.031	< 0.058	< 0.015
M9.75.1M	0.1314	0.071	< 0.031	< 0.058	0.0189
M10.45.1M	0.208	0.042	< 0.031	< 0.058	< 0.015
M10.55.1M	< 0.006	0.0531	< 0.031	< 0.058	0.0284
M10.65.1M	0.204	0.044	< 0.031	< 0.058	< 0.015
M10.75.1M	0.0301	0.0478	< 0.031	0.2203	0.0169
M11.45.1M	0.192	0.041	< 0.031	< 0.058	< 0.015
M11.55.1M	0.173	0.033	< 0.031	< 0.058	< 0.015
M11.65.1M	0.159	0.037	< 0.031	< 0.058	< 0.015
M11.75.1M	0.173	0.039	< 0.031	< 0.058	< 0.015
M12.45.1M	0.192	0.04	< 0.031	< 0.058	< 0.015
M12.55.1M	0.201	0.041	< 0.031	< 0.058	< 0.015
M12.65.1M	0.193	0.048	< 0.031	< 0.058	< 0.015
M12.75.1M	< 0.006	0.0603	< 0.031	< 0.058	< 0.015

Table C-6. (cont'd)

Sample ID	Ni (mg/L)	Pb (mg/L)	Sr (mg/L)	Zn (mg/L)
M5.45.1M	< 0.018	0.085	0.087	0.049
M5.55.1M	< 0.018	0.023	0.133	< 0.025
M5.65.1M	< 0.018	< 0.008	0.149	0.031
M5.75.1M	< 0.018	0.043	0.148	< 0.025
M6.45.1M	< 0.018	0.1175	0.0846	0.0885
M6.55.1M	< 0.018	< 0.008	0.133	0.037
M6.65.1M	< 0.018	0.01	0.127	< 0.025
M6.75.1M	< 0.018	< 0.008	0.123	< 0.025
M7.45.1M	0.019	0.009	0.093	< 0.025
M7.55.1M	< 0.018	< 0.008	0.151	< 0.025
M7.65.1M	< 0.018	< 0.008	0.117	0.027
M7.75.1M	0.038	0.049	0.123	0.051
M8.45.1M	< 0.018	< 0.008	0.132	0.053
M8.55.1M	< 0.018	0.095	0.159	0.028
M8.65.1M	< 0.018	0.056	0.152	< 0.025
M8.75.1M	< 0.018	0.043	0.092	0.071
M9.45.1M	< 0.018	0.1007	0.0801	0.0482
M9.55.1M	< 0.018	0.2056	0.1191	0.0547
M9.65.1M	< 0.018	0.071	0.15	0.041
M9.75.1M	< 0.018	< 0.008	0.137	0.0482
M10.45.1M	< 0.018	< 0.008	0.134	< 0.025
M10.55.1M	< 0.018	0.1434	0.0905	0.0577
M10.65.1M	< 0.018	0.026	0.116	< 0.025
M10.75.1M	< 0.018	0.1503	0.0799	0.0534
M11.45.1M	< 0.018	0.054	0.146	< 0.025
M11.55.1M	< 0.018	0.046	0.133	0.035
M11.65.1M	< 0.018	0.045	0.135	0.029
M11.75.1M	< 0.018	0.01	0.118	< 0.025
M12.45.1M	0.057	0.037	0.081	< 0.025
M12.55.1M	< 0.018	< 0.008	0.14	0.049
M12.65.1M	< 0.018	< 0.008	0.121	0.031
M12.75.1M	< 0.018	< 0.008	0.1041	< 0.025

Table C-6. (cont'd)

Sample ID	Well	Depth	Collection Date	pH (units)	SiO_2 (mg/L)
M13.45.1M	M13	45	09/19/97	7.316	12.4
M13.55.1M	M13	55	09/19/97	7.367	13.8
M13.65.1M	M13	65	09/19/97	7.339	18.5
M13.75.1M	M13	75	09/19/97	7.335	14.1
M14.50.1M	M14	50	09/19/97	7.369	12.9
M14.60.1M	M14	60	09/19/97	7.325	15.4
M14.80.1M	M14	80	09/19/97	7.337	13.9
M14.90.1M	M14	90	09/19/97	7.265	9.2
M15.30.1M	M15	30	09/19/97	7.363	15.0
M15.40.1M	M15	40	09/19/97	7.325	14.2
M15.50.1M	M15	50	09/19/97	7.376	11.8
M15.60.1M	M15	60	09/19/97	7.321	12.4
M15.70.1M	M15	70	09/19/97	7.411	15.4
M15.80.1M	M15	80	09/19/97	7.302	13.5
M15.90.1M	M15	90	09/19/97	7.247	7.7
M16.30.1M	M16	30	09/19/97	7.404	14.6
M16.40.1M	M16	40	09/19/97	7.291	11.3
M16.50.1M	M16	50	09/19/97	7.353	12.5
M16.60.1M	M16	60	09/19/97	7.342	14.2
M16.70.1M	M16	70	09/19/97	7.386	12.6
M16.75.1M	M16	75	09/19/97	7.341	12.8
M16.80.1M	M16	80	09/19/97	7.353	15.1
M16.90.1M	M16	90	09/19/97	7.295	16.4
M17.75.1M	M17	75	09/19/97	7.330	13.4
M18.75.1M	M18	75	09/19/97	7.270	13.1
M19.45.1M	M19	45	09/19/97	7.337	14.3
M19.55.1M	M19	55	09/19/97	7.346	15.1
M19.65.1M	M19	65	09/19/97	7.279	13.2
M19.75.1M	M19	75	09/19/97	7.261	16.9
M20.45.1M	M20	45	09/19/97	7.286	12.3
M20.55.1M	M20	55	09/19/97	7.341	11.4
M20.65.1M	M20	65	09/19/97	7.362	12.8
M20.75.1M	M20	75	09/19/97	7.356	18.7

Table C-6. (cont'd)

Sample ID	Ca (mg/L)	Mg (mg/L)	Na (mg/L)	K (mg/L)
M13.45.1M	90.7	29.4	20.0	7.3
M13.55.1M	99.1	32.0	21.7	3.0
M13.65.1M	98.5	32.6	39.4	3.4
M13.75.1M	100.0	31.3	16.9	2.4
M14.50.1M	85.4	30.6	29.3	5.0
M14.60.1M	115.9	36.1	33.3	4.9
M14.80.1M	103.9	33.2	19.7	1.5
M14.90.1M	101.3	35.1	21.8	3.4
M15.30.1M	103.3	33.5	38.0	5.8
M15.40.1M	101.4	31.2	32.6	6.8
M15.50.1M	64.2	25.1	37.2	1.2
M15.60.1M	94.8	30.2	11.5	3.7
M15.70.1M	112.9	34.1	22.9	1.7
M15.80.1M	97.6	32.4	12.7	2.0
M15.90.1M	80.5	31.3	21.4	0.9
M16.30.1M	95.7	29.9	30.8	4.9
M16.40.1M	70.1	26.0	35.9	4.1
M16.50.1M	84.1	31.1	24.6	4.3
M16.60.1M	100.7	31.6	17.2	2.7
M16.70.1M	87.1	27.8	7.2	2.4
M16.75.1M	87.7	26.7	14.3	1.6
M16.80.1M	101.6	34.5	18.0	1.4
M16.90.1M	113.2	40.3	10.8	3.0
M17.75.1M	94.9	29.8	23.0	5.6
M18.75.1M	102.5	32.1	24.4	5.4
M19.45.1M	95.9	37.8	45.9	4.6
M19.55.1M	107.4	34.6	38.3	4.3
M19.65.1M	108.9	31.7	29.9	3.3
M19.75.1M	131.5	43.3	34.5	1.7
M20.45.1M	87.9	28.8	19.1	6.9
M20.55.1M	79.6	26.5	24.3	1.8
M20.65.1M	98.1	29.2	39.7	3.2
M20.75.1M	99.2	32.7	20.7	2.4

Table C-6. (cont'd)

Sample ID	HCO_3 (mg/L)	Cl (mg/L)	NO_3 (mg/L)	SO_4 (mg/L)
M13.45.1M	397	45.6	42.2	29.6
M13.55.1M	400	35.9	66.6	32.1
M13.65.1M	441	56.4	46.6	26.4
M13.75.1M	413	35.9	50.4	29.7
M14.50.1M	378	76.7	36.1	30.1
M14.60.1M	427	43.6	74.7	29.8
M14.80.1M	400	52.5	67.9	32.8
M14.90.1M	421	59.5	18.7	75.3
M15.30.1M	416	55.5	36.0	22.8
M15.40.1M	444	76.3	34.3	25.9
M15.50.1M	386	69.3	49.7	29.8
M15.60.1M	406	29.2	70.5	31.9
M15.70.1M	400	59.5	65.2	31.1
M15.80.1M	413	37.3	66.6	33.8
M15.90.1M	406	58.8	1.4	85.4
M16.30.1M	386	53.0	32.9	19.7
M16.40.1M	427	62.2	41.4	24.0
M16.50.1M	389	59.2	50.9	29.3
M16.60.1M	375	33.3	59.3	32.3
M16.70.1M	363	44.2	41.5	36.4
M16.75.1M	372	32.3	56.5	34.9
M16.80.1M	381	32.2	66.3	35.4
M16.90.1M	401	47.9	4.8	76.0
M17.75.1M	395	46.9	74.4	35.4
M18.75.1M	429	52.5	73.1	32.1
M19.45.1M	398	58.4	61.5	28.4
M19.55.1M	427	46.1	70.2	28.6
M19.65.1M	453	78.0	46.5	29.2
M19.75.1M	474	69.3	50.1	29.4
M20.45.1M	400	46.3	52.3	28.2
M20.55.1M	407	38.2	70.9	30.7
M20.65.1M	445	64.4	51.1	29.2
M20.75.1M	418	37.6	63.5	30.3

Table C-6. (cont'd)

Sample ID	Al (mg/L)	Ba (mg/L)	Cu (mg/L)	Fe (mg/L)	Mn (mg/L)
M13.45.1M	0.209	0.046	< 0.031	< 0.058	< 0.015
M13.55.1M	0.0394	0.055	< 0.031	< 0.058	0.0217
M13.65.1M	0.224	0.046	< 0.031	0.076	0.078
M13.75.1M	0.21	0.041	< 0.031	< 0.058	0.032
M14.50.1M	0.168	0.045	< 0.031	< 0.058	< 0.015
M14.60.1M	< 0.006	0.0867	< 0.031	< 0.058	< 0.015
M14.80.1M	0.1255	0.058	< 0.031	< 0.058	< 0.015
M14.90.1M	0.275	0.11	< 0.031	0.166	0.169
M15.30.1M	0.1028	0.064	< 0.031	< 0.058	< 0.015
M15.40.1M	0.196	0.051	< 0.031	< 0.058	< 0.015
M15.50.1M	< 0.006	0.047	< 0.031	< 0.058	< 0.015
M15.60.1M	0.183	0.038	< 0.031	< 0.058	< 0.015
M15.70.1M	0.153	0.0693	< 0.031	< 0.058	< 0.015
M15.80.1M	0.225	0.04	< 0.031	< 0.058	< 0.015
M15.90.1M	< 0.006	0.0972	< 0.031	< 0.058	0.1879
M16.30.1M	0.1009	0.0564	< 0.031	< 0.058	< 0.015
M16.40.1M	0.0396	0.0563	< 0.031	< 0.058	0.0396
M16.50.1M	0.2	0.042	< 0.031	< 0.058	< 0.015
M16.60.1M	0.15	0.0561	< 0.031	< 0.058	0.0198
M16.70.1M	0.165	0.032	< 0.031	< 0.058	< 0.015
M16.75.1M	< 0.006	0.0511	< 0.031	< 0.058	0.0226
M16.80.1M	0.1425	0.0631	< 0.031	0.121	0.0551
M16.90.1M	0.384	0.084	< 0.031	0.485	0.484
M17.75.1M	0.175	0.056	< 0.031	< 0.058	< 0.015
M18.75.1M	0.186	0.053	< 0.031	< 0.058	< 0.015
M19.45.1M	< 0.006	0.0688	< 0.031	< 0.058	< 0.015
M19.55.1M	0.0644	0.0777	< 0.031	< 0.058	< 0.015
M19.65.1M	0.189	0.045	< 0.031	< 0.058	< 0.015
M19.75.1M	0.1808	0.0756	< 0.031	< 0.058	< 0.015
M20.45.1M	0.155	0.043	< 0.031	< 0.058	< 0.015
M20.55.1M	< 0.006	0.0482	< 0.031	< 0.058	< 0.015
M20.65.1M	0.209	0.046	< 0.031	< 0.058	< 0.015
M20.75.1M	0.215	0.043	< 0.031	< 0.058	0.038

Table C-6. (cont'd)

Sample ID	Ni (mg/L)	Pb (mg/L)	Sr (mg/L)	Zn (mg/L)
M13.45.1M	< 0.018	0.042	0.117	< 0.025
M13.55.1M	0.0332	0.0693	0.1575	0.0615
M13.65.1M	< 0.018	0.062	0.123	0.03
M13.75.1M	< 0.018	0.044	0.102	< 0.025
M14.50.1M	< 0.018	< 0.008	0.08	< 0.025
M14.60.1M	0.0365	< 0.008	0.1819	0.0284
M14.80.1M	< 0.018	0.0209	0.1094	0.0695
M14.90.1M	< 0.018	< 0.008	0.102	0.032
M15.30.1M	0.0256	< 0.008	0.1935	0.0268
M15.40.1M	< 0.018	0.054	0.163	0.042
M15.50.1M	0.0196	0.1125	0.0671	0.0551
M15.60.1M	0.028	< 0.008	0.154	0.026
M15.70.1M	< 0.018	< 0.008	0.1113	0.0912
M15.80.1M	< 0.018	0.016	0.089	< 0.025
M15.90.1M	< 0.018	0.0779	0.0721	0.0344
M16.30.1M	< 0.018	< 0.008	0.1724	0.0855
M16.40.1M	< 0.018	0.1201	0.1343	0.0665
M16.50.1M	< 0.018	0.12	0.082	0.033
M16.60.1M	0.0242	< 0.008	0.1653	0.0517
M16.70.1M	< 0.018	0.054	0.111	0.033
M16.75.1M	< 0.018	< 0.008	0.0945	0.05
M16.80.1M	0.0181	0.1236	0.0919	0.073
M16.90.1M	< 0.018	0.078	0.089	0.097
M17.75.1M	< 0.018	< 0.008	0.14	0.053
M18.75.1M	< 0.018	< 0.008	0.147	0.054
M19.45.1M	< 0.018	0.0097	0.1042	0.0314
M19.55.1M	0.019	< 0.008	0.1618	0.0419
M19.65.1M	< 0.018	0.025	0.12	0.045
M19.75.1M	< 0.018	< 0.008	0.1273	0.0407
M20.45.1M	< 0.018	< 0.008	0.119	0.032
M20.55.1M	< 0.018	0.086	0.1385	0.0408
M20.65.1M	< 0.018	< 0.008	0.122	< 0.025
M20.75.1M	< 0.018	0.071	0.113	0.042

Table C-6. (cont'd)

Sample ID	Well	Depth	Collection Date	pH (units)	SiO_2 (mg/L)
M23.45.1M	M23	45	09/19/97	7.319	11.8
M23.55.1M	M23	55	09/19/97	7.335	12.4
M23.65.1M	M23	65	09/19/97	7.302	14.7
M23.75.1M	M23	75	09/19/97	7.239	14.4
M24.45.1M	M24	45	09/19/97	7.374	13.4
M24.55.1M	M24	55	09/19/97	7.344	15.8
M24.65.1M	M24	65	09/19/97	7.342	13.3
M24.75.1M	M24	75	09/19/97	7.295	14.7
M25.45.1M	M25	45	09/19/97	7.312	12.4
M25.55.1M	M25	55	09/19/97	7.337	14.8
M25.65.1M	M25	65	09/19/97	7.291	12.7
M25.75.1M	M25	75	09/19/97	7.295	13.2
M26.45.1M	M26	45	09/19/97	7.304	15.1
M26.55.1M	M26	55	09/19/97	7.363	13.0
M26.65.1M	M26	65	09/19/97	7.332	12.4
M26.75.1M	M26	75	09/19/97	7.381	12.7

Table C-6. (cont'd)

Sample ID	Ca (mg/L)	Mg (mg/L)	Na (mg/L)	K (mg/L)
M23.45.1M	82.6	29.8	28.6	5.4
M23.55.1M	95.6	29.0	21.9	4.0
M23.65.1M	117.4	34.5	36.0	2.4
M23.75.1M	112.7	34.6	19.7	2.3
M24.45.1M	89.5	29.3	18.3	2.4
M24.55.1M	107.6	33.6	54.8	3.1
M24.65.1M	92.7	29.4	10.1	3.8
M24.75.1M	97.1	34.9	29.8	7.3
M25.45.1M	89.2	29.2	26.3	5.0
M25.55.1M	106.1	34.1	31.8	4.2
M25.65.1M	103.1	29.6	28.8	2.7
M25.75.1M	102.5	31.9	31.7	2.3
M26.45.1M	105.6	36.8	32.2	16.8
M26.55.1M	89.8	28.8	9.1	3.6
M26.65.1M	98.9	29.3	35.8	2.9
M26.75.1M	87.6	29.0	16.7	2.4

Table C-6. (cont'd)

Sample ID	HCO_3 (mg/L)	Cl (mg/L)	NO_3 (mg/L)	SO_4 (mg/L)
M23.45.1M	395	56.1	61.4	28.6
M23.55.1M	416	47.6	61.7	28.7
M23.65.1M	444	75.1	55.3	29.8
M23.75.1M	471	69.9	56.1	29.3
M24.45.1M	400	34.1	66.7	32.2
M24.55.1M	445	69.9	50.2	28.7
M24.65.1M	383	31.7	72.7	33.1
M24.75.1M	401	55.4	47.9	27.7
M25.45.1M	392	46.6	63.7	27.7
M25.55.1M	413	37.4	78.4	29.1
M25.65.1M	430	68.6	60.4	29.3
M25.75.1M	467	58.4	64.6	29.9
M26.45.1M	401	57.4	46.4	27.8
M26.55.1M	383	35.5	60.1	34.0
M26.65.1M	441	93.2	20.0	27.7
M26.75.1M	389	44.6	53.0	33.4

Table C-6. (cont'd)

Sample ID	Al (mg/L)	Ba (mg/L)	Cu (mg/L)	Fe (mg/L)	Mn (mg/L)
M23.45.1M	0.16	0.039	< 0.031	< 0.058	< 0.015
M23.55.1M	0.155	0.037	< 0.031	< 0.058	< 0.015
M23.65.1M	< 0.006	0.0695	< 0.031	< 0.058	< 0.015
M23.75.1M	0.243	0.04	< 0.031	< 0.058	< 0.015
M24.45.1M	0.174	0.029	< 0.031	< 0.058	< 0.015
M24.55.1M	0.0916	0.0717	< 0.031	< 0.058	0.0304
M24.65.1M	0.178	0.033	< 0.031	< 0.058	< 0.015
M24.75.1M	0.0918	0.0775	< 0.031	< 0.058	< 0.015
M25.45.1M	0.0628	0.0598	< 0.031	< 0.058	< 0.015
M25.55.1M	0.1016	0.0614	< 0.031	< 0.058	< 0.015
M25.65.1M	0.201	0.042	< 0.031	< 0.058	< 0.015
M25.75.1M	0.205	0.041	< 0.031	< 0.058	< 0.015
M26.45.1M	0.0522	0.0828	< 0.031	< 0.058	< 0.015
M26.55.1M	0.167	0.034	< 0.031	< 0.058	< 0.015
M26.65.1M	0.197	0.045	< 0.031	< 0.058	< 0.015
M26.75.1M	0.177	0.033	< 0.031	< 0.058	< 0.015

Table C-6. (cont'd)

Sample ID	Ni (mg/L)	Pb (mg/L)	Sr (mg/L)	Zn (mg/L)
M23.45.1M	< 0.018	0.042	0.086	0.033
M23.55.1M	< 0.018	0.092	0.132	0.057
M23.65.1M	< 0.018	0.0288	0.1262	0.0769
M23.75.1M	< 0.018	0.044	0.103	0.043
M24.45.1M	< 0.018	0.046	0.09	< 0.025
M24.55.1M	< 0.018	< 0.008	0.1406	0.0517
M24.65.1M	< 0.018	< 0.008	0.147	< 0.025
M24.75.1M	0.021	< 0.008	0.1575	0.0295
M25.45.1M	< 0.018	0.1303	0.0982	0.0621
M25.55.1M	< 0.018	0.0131	0.1565	0.0583
M25.65.1M	0.043	0.013	0.11	< 0.025
M25.75.1M	< 0.018	0.058	0.097	0.047
M26.45.1M	< 0.018	< 0.008	0.1596	0.0574
M26.55.1M	< 0.018	0.144	0.146	0.035
M26.65.1M	0.048	< 0.008	0.131	< 0.025
M26.75.1M	< 0.018	0.023	0.088	< 0.025

APPENDIX C

Table C-7. Trace metals concentration when exposed to aquifer solids

Sample location: MW34A
Analysis by: L. Warnick
Analysis date: June 07,1997

	Before Exposure		After Exposure	
	No. Samples	Average	No. Samples	Average
Element	> MDL	(ppm)	> MDL	(ppm)
Al	3	0.019 ± 0.007	3	0.212 ± 0.211
As	0	< 0.05	0	< 0.05
Ba	3	0.097 ± 0.004	0	< 0.002
Cd	0	< 0.004	0	< 0.004
Co	0	< 0.007	0	< 0.007
Cr	0	< 0.007	0	< 0.007
Cu	0	< 0.006	1	0.002
Fe	0	< 0.007	3	0.395 ± 0.291
Mn	0	< 0.002	0	< 0.002
Ni	0	< 0.015	2	0.016 ± 0.007
Pb	0	< 0.040	0	< 0.040
Sr	3	0.146 ± 0.001	3	0.092 ± 0.001
Zn	3	0.727 ± 0.106	1	0.003

Batch experiments (10 mL Schoolcraft groundwater, 1 g solids, time: 3 days)

APPENDIX D

APPENDIX D

BENCH-SCALE COLUMNS

Table D-1. Effluent chemistry for 1-D column (B4)

Absolute PVE	pH	Ca (meq/L)	Mg (meq/L)	Na (meq/L)	K (meq/L)
0.00	7.56	4.50	2.87	1.31	0.18
0.83	7.74	3.14	1.74	3.02	0.16
1.67	7.89	2.13	1.22	3.88	0.15
2.50	7.96	2.10	1.35	4.07	0.16
3.33	8.10	-	-	-	-
4.17	8.16	1.41	2.15	4.08	0.17
5.00	8.23	-	-	-	-
5.83	8.28	0.95	2.51	3.96	0.17
6.67	8.30	-	-	-	-
7.50	8.32	0.91	2.71	3.99	0.18
8.33	8.33	0.90	2.81	4.03	0.18
9.17	8.33	0.88	2.84	4.10	0.18
10.00	8.34	0.87	2.88	4.24	0.18
10.83	8.35	0.88	2.86	4.15	0.19
11.67	8.36	-	-	-	-
12.50	8.39	-	-	-	-
13.33	8.37	0.86	2.79	4.12	0.19

APPENDIX D

Table D-1. (cont'd)

Absolute PVE	pH	SiO_2 (mmol/L)	HCO_3 (meq/L)	Cl (meq/L)	NO_3 (meq/L)	SO_4 (meq/L)
0.00	7.56	0.24	10.05	1.60	0.32	0.42
0.83	7.74	0.21	8.50	1.79	0.37	0.47
1.67	7.89	0.21	-	1.56	0.33	0.40
2.50	7.96	0.22	7.35	1.78	0.37	0.45
3.33	8.10	-	-	-	-	-
4.17	8.16	0.22	8.40	1.95	0.36	0.44
5.00	8.23	-	-	-	-	-
5.83	8.28	0.23	7.55	1.77	0.37	0.45
6.67	8.30	-	-	-	-	-
7.50	8.32	0.22	7.85	-	-	-
8.33	8.33	0.22	-	-	-	-
9.17	8.33	0.23	8.40	-	-	-
10.00	8.34	0.23	-	1.77	0.37	0.45
10.83	8.35	0.23	7.90	1.76	0.37	0.45
11.67	8.36	-	-	-	-	-
12.50	8.39	-	-	-	-	-
13.33	8.37	0.22	7.25	1.73	0.37	0.45

APPENDIX D

Table D-2. Effluent pH for twenty 1-D columns (C-1 to C-20)

Sample	C-1 pH	C-2 pH	C-3 pH	C-4 pH	C-5 pH	C-6 pH	C-7 pH
1	7.55	7.57	7.6	7.55	7.71	7.61	7.6
2	7.72	7.55	7.79	7.53	7.88	7.85	7.81
3	7.94	7.54	7.95	7.55	7.97	7.96	7.92
4	8.09	7.55	8.08	7.55	8.02	8.01	7.98
5	8.19	7.53	8.17	7.53	8.04	8.05	8.01
6	8.25	7.55	8.22	7.52	8.07	8.05	8.02
7	8.28	7.55	8.29	7.53	8.07	8.09	8.04
8	8.29	7.55	8.3	7.53	8.07	8.09	8.06
9	8.31	7.54	8.31	7.54	8.12	8.11	8.1
10	8.32	7.57	8.33	7.54	8.06	8.03	8.03

Sample	C-8 pH	C-9 pH	C-10 pH	C-11 pH	C-12 pH	C-13 pH	C-14 pH
1	7.55	7.54	7.55	7.51	7.45	7.54	7.51
2	7.84	7.73	7.74	7.71	7.58	7.78	7.78
3	7.94	7.87	7.9	7.84	7.77	7.92	7.92
4	8.01	7.94	8.03	7.94	7.84	8.06	8.07
5	8.02	8.1	8.14	8.03	7.86	8.18	8.16
6	8.06	8.19	8.22	8.13	7.95	8.22	8.22
7	8.06	8.23	8.27	8.18	8.03	8.25	8.25
8	8.11	8.24	8.28	8.22	8.06	8.28	8.29
9	8.13	8.26	8.29	8.26	8.09	8.29	8.3
10	8.08	8.28	8.31	8.29	8.13	8.29	8.31

Sample	C-15 pH	C-16 pH	C-17 pH	C-18 pH	C-19 pH	C-20 pH
1	7.69	7.54	7.48	7.68	7.67	7.64
2	7.78	7.68	7.67	7.8	7.85	7.86
3	7.9	7.79	7.84	7.88	7.95	8.04
4	7.94	7.85	7.94	7.94	8.05	8.16
5	8.02	7.92	8.03	7.98	8.14	8.21
6	8.1	7.97	8.09	8.04	8.19	8.25
7	8.15	8	8.15	8.08	8.23	8.28
8	8.21	8.05	8.2	8.12	8.25	8.31
9	8.24	8.06	8.22	8.19	8.27	8.33
10	8.27	8.1	8.24	8.22	8.28	8.34

APPENDIX D

Table D-3. Effluent chemistry for 1-D column (C-29)

Column	Sample	pH	Ca (meq/L)	Mg (meq/L)	Na (meq/L)	K (meq/L)
C-29	1	7.45	3.77	3.13	1.31	0.14
C-29	2	7.65	2.94	1.92	1.61	0.10
C-29	3	7.81	2.49	1.90	1.78	0.11
C-29	4	7.93	2.06	2.53	1.81	0.12
C-29	5	8.03	1.76	2.83	1.79	0.13
C-29	6	8.13	1.63	2.91	1.77	0.13
C-29	7	8.19	1.63	3.02	1.75	0.13
C-29	8	8.26	1.63	2.99	1.79	0.13
C-29	9	8.24	1.56	3.04	1.74	0.12
C-29	10	8.28	1.54	3.02	1.77	0.13
C-29	11	8.28	-	-	-	-
C-29	12	8.31	-	-	-	-
C-29	13	8.32	-	-	-	-
C-29	14	8.32	-	-	-	-
C-29	15	8.33	-	-	-	-

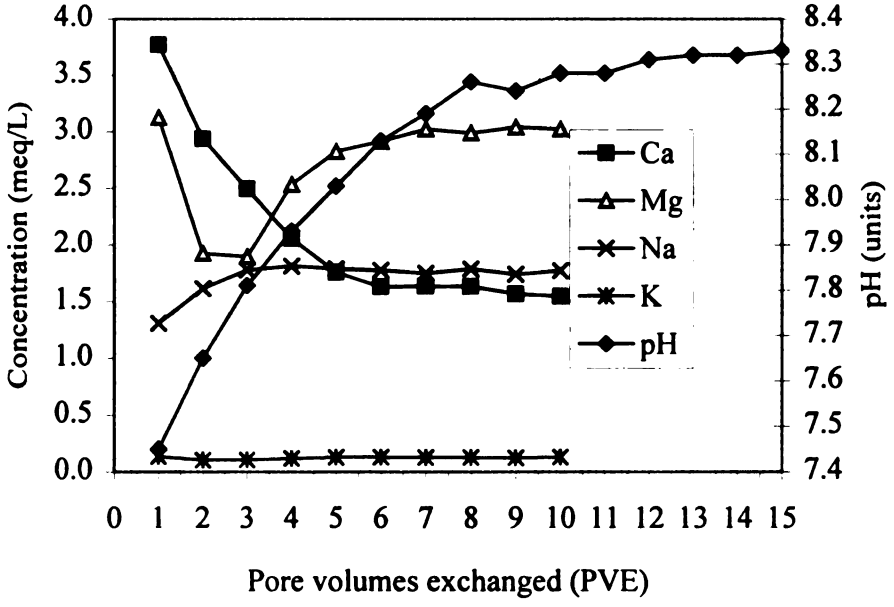

Figure D-1. Effluent chemistry for 1-D column (C-29)

APPENDIX D

Table D-4. Effluent chemistry for 1-D column (C-30)

Column	Sample	pH	Ca (meq/L)	Mg (meq/L)	Na (meq/L)	K (meq/L)
C-30	1	7.47	1.95	2.82	1.27	0.11
C-30	2	7.66	1.73	1.71	1.52	0.09
C-30	3	7.77	1.66	1.45	1.76	0.09
C-30	4	7.86	1.97	1.71	1.71	0.10
C-30	5	7.94	1.56	2.23	1.70	0.10
C-30	6	8.06	1.39	2.41	1.72	0.11
C-30	7	8.13	1.41	2.64	1.75	0.10
C-30	8	8.18	1.43	2.61	1.75	0.11
C-30	9	8.21	1.29	2.66	1.91	0.13
C-30	10	8.25	1.39	2.69	1.75	0.11
C-30	11	8.27	1.33	2.57	1.67	0.12
C-30	12	8.29	1.36	2.78	1.76	0.11
C-30	13	8.29	1.31	2.59	1.67	0.12
C-30	14	8.3	1.30	2.60	1.70	0.11
C-30	15	8.32	1.31	2.63	1.74	0.10

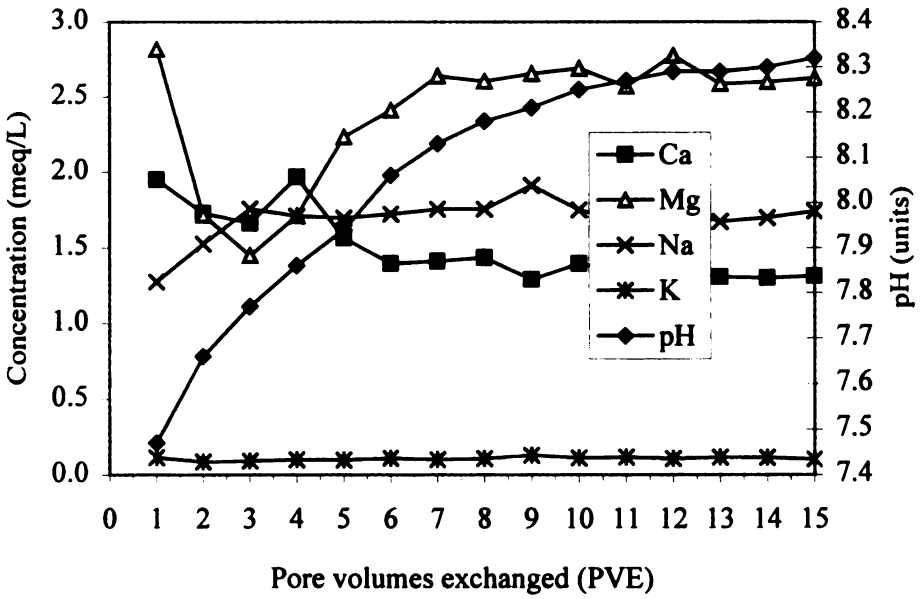

Figure D-2. Effluent chemistry for 1-D column (C-30)

APPENDIX D

Table D-5. Effluent chemistry for 1-D column (C-35)

Column	Sample	pH	Ca (meq/L)	Mg (meq/L)	Na (meq/L)	K (meq/L)
C-35	1	7.41	1.42	2.70	1.34	0.13
C-35	2	7.58	1.90	1.74	1.47	0.11
C-35	3	7.73	1.95	1.45	1.67	0.09
C-35	4	7.8	1.49	1.78	1.97	0.13
C-35	5	7.85	1.73	2.29	1.70	0.12
C-35	6	7.88	1.47	2.39	1.67	0.13
C-35	7	7.95	1.33	2.49	1.68	0.13
C-35	8	7.97	1.33	2.53	1.66	0.12
C-35	9	8.02	1.30	2.57	1.71	0.13
C-35	10	8.01	1.36	2.58	1.88	0.13
C-35	11	8.09	-	-	-	-
C-35	12	8.07	-	-	-	-
C-35	13	8.11	-	-	-	-
C-35	14	8.14	-	-	-	-
C-35	15	8.12	-	-	-	-

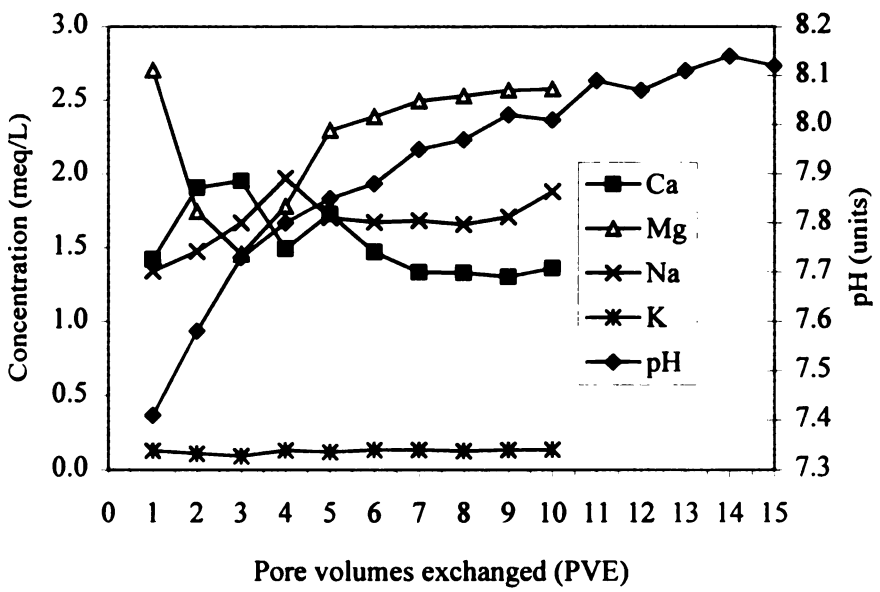

Figure D-3. Effluent chemistry for 1-D column (C-35)

APPENDIX E

APPENDIX E

BASE-ADJUSTED AQUIFER SOLIDS

Table E-1. Base exchange capacity of aquifer solids

Sample	1-D Column	Type	Ca (meq/100 g)	Mg (meq/100 g)	Ca+Mg (meq/100 g)
2-6608-1	1	pH-adjusted	0.87	0.18	1.05
2-6608-2C	2	Control	1.06	0.11	1.18
4-7810-3	3	pH-adjusted	2.02	0.25	2.29
4-7810-4C	4	Control	1.49	0.16	1.66
6-3111-5	5	pH-adjusted	-	-	-
6-3111-5C	5	Control	2.48	0.22	2.71
2-5405-6	6	pH-adjusted	1.51	0.22	1.75
2-5405-6C	6	Control	1.24	0.15	1.39
4-7604-7	7	pH-adjusted	1.52	0.26	1.79
4-7604-7C	7	Control	1.64	0.17	1.82
2-6010-8	8	pH-adjusted	1.60	0.22	1.83
2-6010-8C	8	Control	1.04	0.13	1.18
14-7706-9	9	pH-adjusted	1.47	0.21	1.69
14-7706-9C	9	Control	1.60	0.15	1.76
10-6406-10	10	pH-adjusted	1.28	0.24	1.53
10-6406-10C	10	Control	2.13	0.19	2.33
4-5200-11	11	pH-adjusted	1.65	0.24	1.91
4-5200-11C	11	Control	1.75	0.16	1.92
4-3406-12	12	pH-adjusted	1.84	0.37	2.24
4-3406-12C	12	Control	1.81	0.20	2.03
6-6500-13	13	pH-adjusted	1.63	0.25	1.89
6-6500-13C	13	Control	1.14	0.13	1.28
10-5503-14	14	pH-adjusted	2.27	0.27	2.55
10-5503-14C	14	Control	2.73	0.19	2.93
D10-4500	15	Core	2.83	0.21	2.83
15	15	pH-adjusted	2.44	0.34	2.44
15C	15	Control	2.02	0.19	2.02

APPENDIX E

Table E-1. (cont'd)

Sample	1-D Column	Type	Ca (meq/100 g)	Mg (meq/100 g)	Ca+Mg (meq/100 g)
D4-4706	16	Core	1.25	0.12	1.25
16	16	pH-adjusted	2.42	0.32	2.42
16C	16	Control	2.39	0.20	2.39
D4-4500	17	Core	2.76	0.21	2.76
17	17	pH-adjusted	2.99	0.27	2.99
17C	17	Control	3.18	0.20	3.18
D10-3202	18	Core	0.74	0.15	0.74
18	18	pH-adjusted	1.64	0.47	1.64
18C	18	Control	0.57	0.17	0.57
D4-6604	19	Core	2.15	0.23	2.15
19	19	pH-adjusted	1.29	0.16	1.29
19C	19	Control	1.71	0.16	1.71
D14-6206	20	Core	2.67	0.17	2.67
20	20	pH-adjusted	1.53	0.21	1.53
20C	20	Control	1.83	0.15	1.83
D14-4104	21	Core	4.87	0.26	4.87
21	21	pH-adjusted	3.67	0.26	3.67
21C	21	Control	3.47	0.18	3.47
D8-8110	22	Core	2.72	0.17	2.72
22	22	pH-adjusted	1.92	0.19	1.92
22C	22	Control	2.84	0.17	2.84
D4-6206	23	Core	1.77	0.13	1.77
23	23	pH-adjusted	1.81	0.16	1.81
23C	23	Control	1.88	0.11	1.88
D8-5010	24	Core	3.14	0.19	3.14
24	24	pH-adjusted	2.32	0.27	2.32
24C	24	Control	2.38	0.25	2.38
D2-4600	25	Core	4.85	0.25	4.85
25	25	pH-adjusted	0.44	0.16	0.44
25C	25	Control	0.52	0.10	0.52

APPENDIX E

Table E-1. (cont'd)

Sample	1-D Column	Type	Ca (meq/100 g)	Mg (meq/100 g)	Ca+Mg (meq/100 g)
D8-8406	26	Core	2.32	0.23	2.32
26	26	pH-adjusted	1.99	0.19	1.99
26C	26	Control	-	-	-
D4-3610.1	27	Core	3.48	0.23	3.48
D4-3610.2	27	Core	3.39	0.22	3.39
D4-3610.3	27	Core	2.58	0.23	2.58
27.1	27	pH-adjusted	1.33	0.31	1.33
27.2	27	pH-adjusted	1.63	0.33	1.63
27.3	27	pH-adjusted	1.46	0.34	1.46
27C.1	27	Control	1.24	0.20	1.24
27C.2	27	Control	1.27	0.18	1.27
27C.3	27	Control	1.33	0.18	1.33
D14-6610.1	28	Core	3.13	0.18	3.13
D14-6610.2	28	Core	3.17	0.19	3.17
D14-6610.3	28	Core	2.71	0.19	2.71
28.1	28	pH-adjusted	1.03	0.22	1.03
28.2	28	pH-adjusted	1.53	0.18	1.53
28.3	28	pH-adjusted	1.83	0.19	1.83
28C.1	28	Control	2.09	0.14	2.09
28C.2	28	Control	1.99	0.13	1.99
28C.3	28	Control	2.02	0.15	2.02
D4-5406.1	29	Core	1.45	0.15	1.45
D4-5406.2	29	Core	1.23	0.13	1.23
D4-5406.3	29	Core	1.35	0.12	1.35
29.1	29	pH-adjusted	1.08	0.17	1.08
29.2	29	pH-adjusted	1.19	0.16	1.19
29.3	29	pH-adjusted	1.71	0.18	1.71
29C.1	29	Control	1.14	0.11	1.14
29C.2	29	Control	1.17	0.09	1.17
29C.3	29	Control	1.19	0.11	1.19

APPENDIX E

Table E-1. (cont'd)

Sample	1-D Column	Type	Ca (meq/100 g)	Mg (meq/100 g)	Ca+Mg (meq/100 g)
D6-5006.1	30	Core	1.70	0.15	1.70
D6-5006.2	30	Core	1.69	0.15	1.69
D6-5006.3	30	Core	1.59	0.16	1.59
30.1	30	pH-adjusted	0.97	0.23	0.97
30.2	30	pH-adjusted	1.14	0.29	1.14
30.3	30	pH-adjusted	1.34	0.25	1.34
30C.1	30	Control	1.44	0.13	1.44
30C.2	30	Control	1.57	0.15	1.57
30C.3	30	Control	1.14	0.23	1.14
D6-3702.1	31	Core	0.91	0.16	0.91
D6-3702.2	31	Core	0.99	0.17	0.99
D6-3702.3	31	Core	0.99	0.17	0.99
31.1	31	pH-adjusted	0.86	0.24	0.86
31.2	31	pH-adjusted	0.79	0.24	0.79
31.3	31	pH-adjusted	0.69	0.25	0.69
31C.1	31	Control	0.74	0.14	0.74
31C.2	31	Control	0.79	0.15	0.79
31C.3	31	Control	0.81	0.13	0.81
D4-7206.1	32	Core	1.56	0.17	1.56
D4-7206.2	32	Core	1.63	0.16	1.63
D4-7206.3	32	Core	1.57	0.15	1.57
32.1	32	pH-adjusted	0.97	0.24	0.97
32.2	32	pH-adjusted	0.93	0.24	0.93
32.3	32	pH-adjusted	0.86	0.33	0.86
32C.1	32	Control	0.89	0.12	0.89
32C.2	32	Control	0.89	0.11	0.89
32C.3	32	Control	1.12	0.12	1.12

APPENDIX E

Table E-2. Composition of dissolved pH-adjusted aquifer solids

Cores after 1-D exchanges in 15 cm column
Dissolution of minerals using 1 N HNO_3
Extracted concentrations (mg/g solids)

Sample	1-D Column	Type	Si mg/g	Mn mg/g	Fe mg/g	Mg mg/g	Al mg/g	Ca mg/g	K mg/g
D4-3610.1	27	Core	0.26	0.05	0.38	6.0	0.08	23.4	0.23
D4-3610.2	27	Core	0.39	0.04	0.43	6.5	0.16	24.7	0.67
D4-3610.3	27	Core	0.31	0.04	0.39	5.8	0.08	22.2	0.22
27.1	27	pH-adjusted	0.23	0.03	0.36	6.2	0.18	24.2	0.39
27.2	27	pH-adjusted	0.21	0.03	0.35	6.3	0.17	22.8	0.35
27.3	27	pH-adjusted	0.27	0.03	0.41	6.4	0.12	24.1	0.33
27C.1	27	Control	0.39	0.04	0.38	6.4	0.15	24.6	0.56
27C.2	27	Control	0.20	0.03	0.36	6.2	0.14	22.3	0.38
27C.3	27	Control	0.24	0.03	0.37	6.3	0.18	23.6	0.48
D14-6610	28	Core	0.15	0.01	0.28	5.3	0.22	19.8	0.57
28	28	pH-adjusted	0.15	0.02	0.23	4.7	0.13	17.5	0.35
28C	28	Control	0.15	0.01	0.28	5.9	0.21	20.9	0.50
D4-5406	29	Core	0.19	0.02	0.23	4.2	0.13	18.2	0.34
29	29	pH-adjusted	0.17	0.02	0.23	3.9	0.14	17.7	0.35
29C	29	Control	0.10	0.02	0.21	3.3	0.13	18.0	0.16
D6-5006	30	Core	0.18	0.03	0.29	5.0	0.11	21.2	0.12
30	30	pH-adjusted	0.20	0.00	0.31	5.6	0.28	20.8	0.87
30C	30	Control	0.15	0.02	0.26	4.9	0.20	20.0	0.49
D6-3702	31	Core	0.24	0.04	0.46	8.8	0.17	27.8	0.41
31	31	pH-adjusted	0.35	0.04	0.44	9.5	0.00	30.8	0.54
31C	31	Control	0.28	0.05	0.45	9.6	0.00	31.1	0.32
D4-7206	32	Core	0.23	0.03	0.34	6.4	0.13	21.5	0.26
32	32	pH-adjusted	0.13	0.01	0.23	5.3	0.14	18.4	0.49
32C	32	Control	0.11	0.00	0.16	3.4	0.16	15.4	0.40

APPENDIX F

APPENDIX F

PHREEQC MODELING

Table F-1. PHREEQC input file

```
TITLE Simulation of Schoolcraft Column Experiments
PHASES
        Fixed_pH
        H+ = H+
        log_K  0.0
END
SOLUTION 0 Displacing solution
        pH              8.39
        temp            25.0
        -units          ppm
        Ca              17.1
        Mg              33.9
        Na              94.7
        K               7.3
        Alkalinity      442
        Cl              61.4
        N(5)            22.8
        S(6)            21.5
        Si              13.5
END
SELECTED_OUTPUT
        -file           110803.pun
        -totals         Ca Mg Na K
        -si             Calcite Dolomite Quartz
END
SOLUTION 1 Initial solution in pore volume
        pH              7.56
        temp            25.0
        -units          ppm
        Ca              90.1
        Mg              34.9
        Na              30.2
        K               7.0
```

Table F-1. (cont'd)

```
        Alkalinity      613
        Cl              56.8
        N(5)            20.12
        S(6)            20.2
        Si              14.2
EXCHANGE 1
#       Exch.           Amount
        CaX2            0.0055
        MgX2            0.0011
USE exchange none
SURFACE 1
#       Surf.           Amount      Area    Mass
        Hfo_w           0.0025      600.    30.
USE surface none
END
TRANSPORT
        -cells  1
        -shifts 15
END
```

APPENDIX F

Table F-2. PHREEQC saturation indices for pore solution

Phase	SI	log IAP	log KT	Formula
Anhydrite	-2.54	-6.9	-4.36	CaSO4
Aragonite	0.68	-7.66	-8.34	CaCO3
Brucite	-4.81	12.03	16.84	Mg(OH)2
Calcite	0.82	-7.66	-8.48	CaCO3
Chalcedony	-0.08	-3.63	-3.55	SiO2
Chrysotile	-3.37	28.83	32.2	Mg3Si2O5(OH)4
Clinoenstatite	-2.94	8.4	11.34	MgSiO3
CO2(g)	-1.72	-19.87	-18.15	CO2
Cristobalite	-0.04	-3.63	-3.59	SiO2
Diopside	-2.91	16.99	19.89	CaMgSi2O6
Dolomite	1.59	-15.5	-17.09	CaMg(CO3)2
Dolomite(d)	1.04	-15.5	-16.54	CaMg(CO3)2
Epsomite	-4.95	-7.09	-2.14	MgSO4:7H2O
Fixed_pH	-7.56	-7.56	0	H+
Forsterite	-7.88	20.43	28.31	Mg2SiO4
Gypsum	-2.32	-6.9	-4.58	CaSO4:2H2O
H2(g)	-23.12	-23.12	0	H2
Halite	-7.37	-5.79	1.58	NaCl
Huntite	-1.21	-31.18	-29.97	CaMg3(CO3)4
Magadiite	-6.47	-20.77	-14.3	NaSi7O13(OH)3:3H2O
Magnesite	0.19	-7.84	-8.03	MgCO3
Nahcolite	-4.37	-15.25	-10.88	NaHCO3
Natron	-9.31	-10.62	-1.31	Na2CO3:10H2O
Nesquehonite	-2.22	-7.84	-5.62	MgCO3:3H2O
O2(g)	-36.88	46.24	83.12	O2
Portlandite	-10.59	12.21	22.8	Ca(OH)2
Quartz	0.35	-3.63	-3.98	SiO2
SiO2(a)	-0.92	-3.63	-2.71	SiO2
Talc	0.18	21.58	21.4	Mg3Si4O10(OH)2
Thenardite	-9.69	-9.87	-0.18	Na2SO4
Thermonatrite	-10.75	-10.62	0.12	Na2CO3:H2O

APPENDIX F

Table F-3. PHREEQC saturation indices for displacing solution

Phase	SI	log IAP	log KT	Formula
Anhydrite	-3.17	-7.53	-4.36	CaSO4
Aragonite	0.64	-7.7	-8.34	CaCO3
Brucite	-3.15	13.69	16.84	Mg(OH)2
Calcite	0.78	-7.7	-8.48	CaCO3
Chalcedony	-0.11	-3.66	-3.55	SiO2
Chrysotile	1.53	33.73	32.2	Mg3Si2O5(OH)4
Clinoenstatite	-1.32	10.02	11.34	MgSiO3
CO2(g)	-2.7	-20.85	-18.15	CO2
Cristobalite	-0.08	-3.66	-3.59	SiO2
Diopside	-0.38	19.51	19.89	CaMgSi2O6
Dolomite	2.23	-14.86	-17.09	CaMg(CO3)2
Dolomite(d)	1.68	-14.86	-16.54	CaMg(CO3)2
Epsomite	-4.86	-7	-2.14	MgSO4:7H2O
Fixed_pH	-8.39	-8.39	0	H+
Forsterite	-4.6	23.71	28.31	Mg2SiO4
Gypsum	-2.95	-7.53	-4.58	CaSO4:2H2O
H2(g)	-24.78	-24.78	0	H2
Halite	-6.83	-5.25	1.58	NaCl
Huntite	0.78	-29.19	-29.97	CaMg3(CO3)4
Magadiite	-5.39	-19.69	-14.3	NaSi7O13(OH)3:3H2O
Magnesite	0.87	-7.16	-8.03	MgCO3
Nahcolite	-4.02	-14.89	-10.88	NaHCO3
Natron	-7.63	-8.94	-1.31	Na2CO3:10H2O
Nesquehonite	-1.54	-7.16	-5.62	MgCO3:3H2O
O2(g)	-33.56	49.56	83.12	O2
Portlandite	-9.65	13.15	22.8	Ca(OH)2
Quartz	0.32	-3.66	-3.98	SiO2
SiO2(a)	-0.95	-3.66	-2.71	SiO2
Talc	5	26.4	21.4	Mg3Si4O10(OH)2
Thenardite	-8.6	-8.78	-0.18	Na2SO4
Thermonatrite	-9.07	-8.94	0.12	Na2CO3:H2O

APPENDIX F

Table F-4. PHREEQC selected output file

step	ph	Ca	Mg	Na	K	Calcite _si	Dolomite _si	Quartz _si
-99	7.560	2.25E-03	1.44E-03	1.31E-03	1.79E-04	0.824	1.593	0.354
1	7.987	1.02E-03	4.70E-04	3.54E-03	1.02E-04	0.792	1.387	0.327
2	8.020	9.95E-04	7.00E-04	4.06E-03	1.52E-04	0.805	1.598	0.326
3	8.083	8.75E-04	8.35E-04	4.11E-03	1.70E-04	0.809	1.740	0.325
4	8.143	7.85E-04	9.41E-04	4.11E-03	1.79E-04	0.819	1.860	0.324
5	8.197	7.15E-04	1.03E-03	4.12E-03	1.83E-04	0.829	1.960	0.323
6	8.242	6.61E-04	1.10E-03	4.12E-03	1.85E-04	0.837	2.041	0.321
7	8.279	6.18E-04	1.16E-03	4.12E-03	1.85E-04	0.842	2.102	0.320
8	8.307	5.82E-04	1.20E-03	4.12E-03	1.86E-04	0.843	2.148	0.319
9	8.329	5.54E-04	1.24E-03	4.12E-03	1.86E-04	0.841	2.180	0.319
10	8.345	5.30E-04	1.27E-03	4.12E-03	1.86E-04	0.837	2.201	0.318
11	8.357	5.11E-04	1.30E-03	4.12E-03	1.86E-04	0.831	2.215	0.318
12	8.366	4.95E-04	1.32E-03	4.12E-03	1.87E-04	0.826	2.224	0.317
13	8.372	4.83E-04	1.33E-03	4.12E-03	1.87E-04	0.820	2.229	0.317
14	8.377	4.72E-04	1.34E-03	4.12E-03	1.87E-04	0.815	2.232	0.317
15	8.380	4.64E-04	1.35E-03	4.12E-03	1.87E-04	0.810	2.234	0.317

REFERENCES

APHA, AWWA, and WEF. 1992. Standard methods for the examination of water and wastewater. American Public Heath Association, Washington, DC.

Appelo, C. A. J., A. Willemsen, H. E. Beekman, and J. Griffioen. 1990. Geochemical calculations and observations on salt water intrustions. II. Validation of a geochemical model with laboratory experiments. Journal of Hydrology, v. 120 pp. 225-250.

Appelo, C. A. J. 1994. Cation and proton exchange, pH variations, and carbonate reactions in a freshening aquifer. Water Resources Research, v. 30, no. 10, pp. 2793-2805.

ASTM. 1996. Annual book of ASTM standards. American Society for Testing and Materials, West Conshohocken, PA.

Criddle, C. S., J. T. DeWitt, D. Grbic-Galic, and P. L. McCarty. 1992. Transformation of cabon tetrachloride by *Pseudomonas* sp. strain KC under denitrifying conditions. Applied and Environmental Microbiology. v. 56, no. 11, pp. 3240-3246.

Drever, J. I. 1997. The geochemistry of natural waters: surface and groundwater environments. Prentice-Hall, Upper Saddle River, NJ. 436 pp.

Dybas, M. J., G. M. Tatara, and C. S. Criddle. 1995. Localization and characterization of carbon tetrachloride transformation activity of *Pseudomonas* sp. strain KC. Applied and Environmental Microbiology, v. 61, pp. 758-762.

Freeze, R. A. and J. A. Cherry, 1979. Groundwater. Prentice-Hall, Englewood Cliffs, NJ. 604 pp.

Griffioen, J. 1993. Multicomponent cation exchange including alkalinization/ acidification following flow through sandy sediment. Water Resources Research. v. 29, no. 9, pp. 3005-3019.

Lewis, T. A. and R. L. Crawford. 1993. Physiological factors affecting carbon tetrachloride dehalogenation by the denitrifying bacterium *Pseudomonas* sp. strain KC. Applied and Environmental Microbiology, v. 59, no. 5, pp.1635-1641.

Mayotte, T. J., M. J. Dybas, and C. S. Criddle. 1996. Bench-scale evaluation of bioaugmentation to remediate carbon tetrachloride-contaminated aquifer materials. Ground Water, v. 34, no. 2, pp. 358-367.

McBride, M. 1994. Environmental chemistry of soils. Oxford University Press, New York NY.

NCR. 1988. Recommended chemical soil test procedures for the North Central Region. North Central Regional Pulication No. 221 (Revised), Bulletin No. 499 (Revised).

NRC. 1990. Ground water models: scientific and regulatory applications. National Research Council (U.S.), Committee on Ground Water Modeling Assessment. National Academy of Sciences, Washington, DC.

Parkhurst, D. L. 1995. User's guide to PHREEQC—a computer program for speciation, reaction-path, advective-transport, and inverse geochemical calculations. U. S. Geological Survey. Water-Resources Investigations Report 95-4227.

Pratt, P. F. 1961. Effect of pH on the cation-exchange capacity of surface soils. Proceedings of the Soil Science Society of America. v. 25, no. 2, pp. 96-98.

Schoolcraft Field Bioaugmentation Experiment. 1997. Evaluation of *in-situ* bioaugmentation to remediate an aquifer contaminated with carbon tetrachloride. Technical Report #4.

Sibley, D. 1997. Characterization of minerals. [Online] Available email: warnickl@pilot.msu.edu from sibley@pilot.msu.edu, March 27, 1997.

Snoeyink, V. L. and D. Jenkins. 1980. Water Chemistry. John Wiley. New York

SSSA. 1986. Methods of soil analysis, part 1, physical and mineralogical methods. Soil Science Society of America, Madison WI.

Sullivan, P. J. 1977. The principle of hard and soft acids and bases as applied to exchangeable cation selectivity in soils. Proceedings of the Soil Science Society of America. v. 124, pp. 117-121.

Tatara, G. M., M. J. Dybas, and C. S. Criddle. 1993. Effects of medium and trace metals on kinetics of carbon tetracloride transformation by *Pseudomonas*

sp. strain KC. Applied and Environmental Microbiology. v. 49, pp. 2126-2131.

Ulrich, B., and M. E. Sumner. 1991. Soil acidity. Springer-Verlag, Berlin, Germany.

USGS. 1996. Geohydrology and water quality of Kalamazoo County, Michigan, 1986-88. U. S. Geological Survey. Water-Resources Investigations Report 90-4028.

Wahrer, M. A. 1993. The geochemistry and source of solutes in ground water from the Glacial Drift Regional Aquifer, Michigan Basin. Thesis, Michigan State University.